



MIT Open Access Articles

Proteomic characterization of human multiple myeloma bone marrow extracellular matrix

The MIT Faculty has made this article openly available. **Please share** how this access benefits you. Your story matters.

Citation	Glavey, S. V. et al. "Proteomic Characterization of Human Multiple Myeloma Bone Marrow Extracellular Matrix." <i>Leukemia</i> 31, 11 (March 2017): 2426–2434
As Published	https://doi.org/10.1038/leu.2017.102
Publisher	Nature Publishing Group
Version	Author's final manuscript
Citable link	http://hdl.handle.net/1721.1/117210
Terms of Use	Article is made available in accordance with the publisher's policy and may be subject to US copyright law. Please refer to the publisher's site for terms of use.

36 **ABSTRACT**

37

38 The extracellular matrix (ECM) is a major component of the tumor microenvironment,
39 contributing to the regulation of cell survival, proliferation, differentiation and metastasis. In
40 multiple myeloma (MM), interactions between MM cells and the bone marrow (BM)
41 microenvironment, including the BM ECM, are critical to the pathogenesis of the disease and
42 the development of drug resistance. Nevertheless, composition of the ECM in MM and its
43 role in supporting MM pathogenesis has not been reported. We have applied a novel
44 proteomic-based strategy and defined the BM ECM composition in patients with monoclonal
45 gammopathy of undetermined significance (MGUS), newly diagnosed and relapsed MM
46 compared to healthy donor-derived BM ECM. In this study, we show that the tumor ECM is
47 remodeled at the mRNA and protein level in MGUS and MM to allow development of a
48 permissive microenvironment. We further demonstrate that two ECM-affiliated proteins,
49 ANXA2 and LGALS1, are more abundant in MM and high expression is associated with a
50 decreased overall survival. This study points to the importance of ECM remodeling in MM
51 and provides a novel proteomic pipeline for interrogating the role of the ECM in cancers with
52 BM tropism.

53

54 **Keywords: Multiple Myeloma, Extracellular Matrix, Proteomics**

55

56

57

58

59

60

61

62

63

64

65

66

67

68

69 **INTRODUCTION**

70

71 Multiple myeloma (MM) is a plasma cell malignancy and accounts for approximately 10% of
72 all hematological cancers (1). MM provides a model for the study of cancer cell metastasis as
73 MM cells are known to traffic to distant bone marrow (BM) niches via hijacking the normal
74 processes of cellular metastasis (2). Progression of the disease is mediated by intrinsic factors
75 of the clonal cells along with factors that mediate a permissive tumor microenvironment (3).
76 The MM tumor niche comprises the components of the BM microenvironment - cellular
77 (stromal cells, osteoblasts, osteoclasts, endothelial cells and immune cells) and non-cellular
78 (ECM) (4, 5). Despite advances in therapies in recent years, MM remains an incurable
79 disease with a median survival of approximately 5-7 years for newly diagnosed patients (6).
80 Identification of the molecular mechanisms leading to MM has the potential to lead to the
81 development of novel prognostic tests and therapies for MM patients (7)(8).

82

83 The extracellular matrix (ECM) is a complex meshwork of proteins that serves as a scaffold
84 for cells. In addition, it actively participates in cell functions such as proliferation, migration
85 and survival via cell-to-matrix interactions (9, 10). The ECM is also rich in growth factors
86 and cytokines thus supporting cell biology (9); therefore it follows that alterations in the
87 ECM may be expected to occur in disease states such as inflammation and cancer. This is
88 indeed the case in several tumor types where ECM alterations have been associated with
89 changes in metastatic potential of tumor cells *in vivo* and in clinical outcomes (11, 12). The
90 role of the ECM as a metabolic regulator of cell function also has implications for malignant
91 processes (13) and molecular signals of metastasis have implicated ECM components and
92 their receptors in tumor progression (14). In the past, attempts to systematically characterize
93 the ECM were challenged by the vast diversity and number of ECM proteins and also by
94 their insolubility and cross-linked nature. A new perspective on analysis of the ECM, on a
95 relatively high throughput scale, came with the definition and *in-vivo* characterization of the
96 “matrisome” (8). The term “matrisome”, initially used by Martin and collaborators in 1984
97 was updated and refined by Naba et al in 2012. This study revealed tissue specific signatures
98 of ECM proteins and importantly provided a method to determine the origin (tumor cell or
99 stroma) of individual matrix proteins.

100 This, more in-depth knowledge of the ECM composition, was facilitated by whole genome
101 sequencing. This was made possible due to the fact that ECM proteins are encoded by one or
102 a few exons in the genome and whole genome sequencing has therefore provided a platform
103 from which the ECM can be more clearly defined. Bio-informatic analysis of the proteome,

104 using a list of approximately 50 domains to identify a list of candidate ECM proteins, has
105 facilitated the definition of ECM proteins into a more complete list, which has been named
106 the “core matrisome” – in mammals this comprises approximately 300 proteins. These
107 proteins include large insoluble proteins such as collagens, proteoglycans and glycoproteins
108 (15). In addition to these insoluble proteins, there are large numbers of ECM-modifying
109 enzymes, ECM-binding growth factors, and other ECM-associated proteins, which for the
110 most part are soluble in nature. These proteins have been included in a defined category of
111 “matrisome-associated” proteins due to the integral role that they play in ECM function (15) .
112 These different categories of ECM and ECM-associated proteins cooperate to assemble and
113 remodel the matrix and bind to cells through ECM receptors. Together with receptors for
114 ECM-bound growth factors, they serve to control survival, proliferation, differentiation,
115 shape, polarity, and motility of cells (15).

116 This method of ECM profiling has yielded important insights into the composition of several
117 solid tumor matrices along with potential novel therapeutic and prognostic targets (11, 16)
118 however, this method has not been applied to hematological malignancies, where the process
119 of cell migration from the primary niche is largely dependent on the tumor microenvironment
120 (17-19). We characterize the unique extracellular matrices of patients with the pre-myeloma
121 condition monoclonal gammopathy of undetermined significance (MGUS), newly diagnosed
122 and relapsed MM patients and compare them to that of healthy human bone marrow. Our
123 results demonstrate ECM remodeling with disease progression and identify ANXA2 and
124 LGALS1 as ECM proteins that have prognostic relevance for MM patient overall survival.

125

126

127

128

129

130

131

132

133

134

135 **MATERIALS AND METHODS**

136

137 **Human bone marrow aspirates.** Informed consent was obtained from all patients in
138 accordance with the Declaration of Helsinki. These studies were approved by the Dana-
139 Farber Cancer Institute Institutional Review Board and the University of Torino, Italy. Whole
140 bone marrow (BM) was obtained from healthy human donors (n=10), MGUS patients (n=3),
141 newly diagnosed MM patients who had not yet received treatment (n=7) and patients with
142 relapsed MM (n=6). Fresh BM samples (20ml/patient) were filtered and underwent red cell
143 lysis, followed by centrifugation at 2500rpm for 10 minutes (see Supplementary Methods for
144 full protocol). The isolated pellet was then processed through the sequential extraction
145 methods outlined below.

146

147 **Murine models and staining for collagen.**

148 Tumors were established in mice using MM1s-GFP-Luc⁺ cells (5×10^6 / mouse), which were
149 injected into the tail vein of SCID-Bg mice. Mice were sacrificed at 21 days post injection of
150 tumor cells, femurs harvested and staining for collagens performed using Masson's trichrome
151 stain as a surrogate marker for ECM proteins.

152 **ECM protein enrichment and SDS gradient gel separation.** ECM protein enrichment from
153 of whole BM samples was achieved by sequentially depleting intracellular proteins as
154 previously described (8, 20). In brief, whole BM samples were homogenized and subjected to
155 incubations in different buffers to remove (1) cytosolic proteins, (2) nuclear proteins, (3)
156 membrane proteins and (4) cytoskeletal proteins, leaving a final insoluble fraction enriched
157 for ECM proteins.

158

159 **Immunoblotting.** For validation of the extraction process, the different fractions were
160 separated on SDS-polyacrylamide gradient gels, transferred to nitrocellulose membranes and
161 probed with relevant subcellular compartmental antibodies to confirm elimination of
162 intracellular proteins and enrichment of ECM proteins. The antibodies used for
163 immunoblotting included anti-GAPDH, anti-Histone (Cell Signaling Technology, Danvers,
164 MA), anti-transferrin (Invitrogen, Camarillo, CA), anti-vimentin (Cell Signaling Technology,
165 Danvers, MA), anti-fibronectin (Abcam, Cambridge, MA), anti-actin (Santa Cruz
166 Biotechnology, Dallas, TX) or anti- α -tubulin (Cell Signaling Technology, Danvers, MA).

167

168 **Protein digestion in peptides.** The ECM-enriched protein fractions obtained after
169 decellularization were solubilized and reduced in a solution of 8M urea in 100mM

170 ammonium bicarbonate containing 10mM dithiotreitol at 37°C for 30 minutes. The
171 solubilized ECM proteins were then separated on 4-20% SDS-polyacrylamide gradient gels.
172 Gels were stained with Gel Code Blue (Thermo Scientific) and washed in dH₂O. Gels were
173 then cut into 2 or 3 pieces using a clean scalpel and gel pieces were transferred into clean
174 microcentrifuge tubes. Gel bands were wash twice with 200mL of 50% acetonitrile for 15
175 min. Protein gel samples were reduced with 10mM DTT, alkylated with 55mM
176 iodoacetamide and digested overnight with 100ng of sequencing grade TPCK modified
177 trypsin (Promega) at pH=8.3. Samples were acidified with 0.5% trifluoroacetic acid and
178 desalted using C18 zip tips (Millipore) and concentrated to 10uL.

179

180 **Liquid chromatography and Tandem Mass Spectrometry.** 2 to 4uL of peptides were
181 analyzed by microcapillary liquid chromatography (C18) tandem mass spectrometry (LC-
182 MS/MS) using an EASY-nLCII nanoflow HPLC (Thermo Fisher Scientific) coupled to a
183 hybrid Orbitrap Elite high-resolution mass spectrometer (Thermo Fisher Scientific) in Top 6
184 data-dependent acquisition positive ion mode at a flow rate of 300 nL/min. Please see
185 supplemental methods for further information.

186

187 **Protein and peptide identification.** The LC-MS/MS datasets were analyzed with the
188 Spectrum Mill software package, v 5.0 pre-release (Agilent Technologies, Santa Clara, CA).
189 MS/MS spectra were searched against UniProt databases containing reference proteome
190 sequences (including isoforms and excluding fragments) downloaded from the UniProt web
191 site on October 17, 2014. Redundant sequences were removed, and a set of common
192 laboratory contaminant proteins (150 sequences) was appended. The human database
193 comprised 59,079 entries. Search criteria, described in the Supplementary Methods, yielded
194 target-decoy-based false-discovery rate estimates for each patient's dataset of <0.8% at the
195 peptide-spectrum match level and <1.3 % at the distinct peptide level. Across all datasets
196 together the peptide-level FDR was 1.9%. Peptide-spectrum matches from all datasets
197 together were assembled into proteins, and each protein was annotated as ECM-derived or
198 not, as previously described (8, 21). The original mass spectra may be downloaded from
199 MassIVE (<http://massive.ucsd.edu>) using the identifier: MSV000080451. The data is directly
200 accessible via <ftp://massive.ucsd.edu/MSV000080451>.

201

202

203 **Analysis of gene expression profiling and survival analysis.** Publicly available gene
204 expression profiles (GEP) were analyzed to evaluate the expression level of ANXA2 and
205 LGALS1 in MM patient samples and cell lines (GSE6477)(22). We used the Cancer Cell
206 Line Encyclopedia (CCLE) database (<http://www.broadinstitute.org/ccle/home>)(23) to
207 determine the expression level of ANXA2 and LGALS1 across over 1,000 cell lines,
208 expressed by Robust Multi-array Average (RMA) values. We further studied GEP to assess
209 the differential expression of ANXA2 and LGALS1 in MM vs. normal plasma cells –
210 GSE6477. Gene levels were expressed by normalized expression values and 2-tailed t test
211 were calculated to compare the 2 groups. Finally, we analyzed a large GEP - GSE2658 (24) –
212 that enrolled 350 patients at diagnosis of MM. A Kaplan-Meier analysis was performed to
213 compare overall survival (OS) of patients with low vs. high expression level of ANXA2 or
214 LGALS1 based on the median expression of the cohort.

215

216 **Gene set enrichment analysis (GSEA).** We performed gene set enrichment analysis
217 (GSEA)(25) to determine whether the identified ECM gene sets followed the same pattern at
218 the mRNA level in MM patients compared to healthy donors. GSEA was performed
219 following the developer's protocol (<http://www.broad.mit.edu/gsea/>) using the GSEA6477
220 dataset (22).

221

222 **RESULTS**

223

224 **ECM protein enrichment from normal and diseased whole bone marrow samples.**

225 We have examined murine and human BM, using Masson's trichrome to stain fibrillar
226 collagens, as an assessment of ECM content (Fig. 1 and 2). We identified ECM within
227 healthy murine BM niches and observed that the normal architecture of the ECM became
228 disorganized in MM murine bone marrow but was still clearly present (Fig. 1A and B).
229 Similarly, ECM was also identifiable within the BM of MM patients (Fig. 2 A and B), where
230 morphology most resembled that seen in the MM murine BM. In order to isolate and
231 characterize this ECM, we developed a protocol based on the previous decellularization
232 method devised by Naba et al (8) specifically tailored to enrich for insoluble ECM proteins
233 from the liquid marrow (Fig. 3A). Antibody markers, including anti-GAPDH, -histone, -
234 transferrin receptor, and -vimentin were used for the cytosolic, nuclear, membrane and
235 cytoskeletal compartments in order to confirm depletion of intracellular components at each
236 step (Fig. 3B, left panel). In addition, we used an anti-fibronectin antibody to monitor the
237 behavior of one exemplary ECM protein during the decellularization of bone marrow
238 samples. Although we observed a portion of fibronectin to be partially depleted at each step,
239 it was present in the final fraction (Fig. 3B, left panel). The protein fraction that remains
240 insoluble after decellularization was then separated using gel electrophoresis, gels were
241 stained using Coomassie blue stain (Fig. 3B, right panel). Gel bands were further cut from the
242 gels and proteins were subjected to in-gel protein digestion to generate peptides to be
243 separated by liquid chromatography and analyzed by mass spectrometry.

244

245 **Proteomic characterization of healthy human donor, MGUS and MM ECM.**

246 We aimed to define the proteomic signature of BM ECMs obtained from patients with
247 MGUS and MM, as compared to healthy donors-derived BM ECMs. Complete data acquired
248 on independent samples from healthy donors, MGUS patients and MM patients is shown in
249 Supplementary Table S3. Peptide abundance, spectral count, number of unique peptides and
250 number of proteins identified within the whole bone marrow were measured for both healthy
251 donors and patients with MGUS or MM, either at first diagnosis or at relapse (Supplementary
252 Fig. S1). In a representative healthy donor-derived sample, 24% of total spectral count
253 signals were core matrisome or matrisome associated with 43% of the total precursor-ion
254 intensity corresponding to proteins defined as ECM (Fig. S1A). A similar pattern was
255 demonstrated for MGUS, newly diagnosed and relapsed MM BM ECMs (Fig. S1B-D. and

256 Supplementary Table S3B-E). In previous studies conducted on solid tumors (melanoma or
257 mammary tumor xenografts, and human metastatic colorectal carcinomas), we have reported
258 that the majority, typically (>75%) of the total precursor-ion intensities, correspond to
259 matrisome proteins (8, 11, 16). This may indicate that the bone marrow ECM is comprised of
260 a larger fraction of soluble ECM components, which by their nature are more readily
261 extractable during the decellularization process than the ECM of normal tissues and solid
262 tumors, where the ECM may play a greater structural role, and therefore be higher in in-
263 soluble components. In addition, it is worth noting that the inter-patient variability was
264 greater than what we previously observed in solid tumor ¹¹. Starting with 20 ml of bone
265 marrow aspirate for each donor or patient, we observed that the proportion of the total
266 precursor-ion intensities corresponding to matrisome proteins ranged from 10% to nearly
267 50%, (see Supplementary Fig. S2 and Supplementary Table S3A).

268

269 **Characterization of the matrisome from healthy donor bone marrow.**

270 We defined the matrisome of healthy-donor-derived BM as the ensemble of proteins detected
271 in at least three independent biological replicates (i.e. patients) and by at least three peptides
272 in one of the replicates. According to this definition the BM ECM from 10 independent
273 healthy donors was composed of 62 proteins (Supplementary Table S1A). We previously
274 proposed to classify proteins as part of the core matrisome, which comprises ECM
275 glycoproteins, collagens, and proteoglycans, or being matrisome-associated proteins (ECM-
276 affiliated proteins, ECM regulators, and ECM-associated secreted factors) (8, 21). The human
277 bone marrow matrisome comprises 30 core matrisome proteins and 32 matrisome-associated
278 proteins (Supplementary Table S1A, Supplementary Table S3B). The interrogation of the
279 MatrisomeDB database (21) further revealed the identification of 11 proteins that have not
280 been previously detected in any of the human tissues included in the database
281 (Supplementary Table S1A). As human BM has not been previously subjected to this type of
282 method, these proteins may be specific to this tissue.

283

284 **Characterization of the matrisome from MGUS and MM patients.**

285 We next sought to define the proteomic signature for BM ECMs derived from MGUS
286 patients, using the same criteria outlined above, and found 11 proteins, two of which were
287 core matrisome proteins, namely Bone Marrow Proteoglycan 2 (PRG2) and Bone Marrow
288 proteoglycan 3 (PRG3) (Supplementary Table S1B). Nine of the proteins identified in the
289 MGUS patient bone marrows were matrisome associated, including the ECM-affiliated

290 protein ficolin 1 (FCN1), the ECM-remodeling enzymes CTSG, Serpins, and the secreted
291 factors HRNR, S100A8 and S100A9 (Supplementary Table S1B).

292 Analysis of the ECM signature of MM bone marrow identified 32 proteins (Supplementary
293 Table S1C). Ten of these proteins were core matrisome proteins, with 22 being matrisome
294 associated. Interestingly two matrisome associated proteins were identified, Annexin A2
295 (ANXA2) and Galectin-1 (LGALS1), which were not identified in healthy donor or MGUS
296 bone marrow. The ECM of patients with relapsed MM comprised of 25 proteins, 10 of which
297 are core matrisome proteins and 15 of which are matrisome associated (Supplementary Table
298 S1D).

299

300 **The analysis of the ECM identified signatures of MGUS and progressive MM.**

301 By comparing the matrisomes of healthy donor bone marrow, MGUS and progressive stages
302 of MM, we identified 11 proteins expressed by all four groups (Fig. 4A-B). Examples of
303 these proteins are cathepsin-G (CTSG) and neutrophil elastase (ELANE). We further
304 remarked that the normal-bone-marrow matrisome contained more proteins than diseased
305 bone marrow samples. Because the proteomic pipeline employed analyzed only proteins that
306 remained insoluble after decellularization, one hypothesis is that the ECM proteins in MGUS
307 or MM bone marrow samples are more soluble. In agreement with this hypothesis, we
308 observed the loss of several collagens and other fibrillar ECM glycoproteins such as
309 fibronectin in MGUS and MM samples (Supplementary Table S2, Supplementary Table
310 S3B-E). We also observed that some collagens and matrix metallo-proteinases (MMPs)
311 found in healthy donor bone marrow and not detected at the MGUS stage are detected later in
312 the disease progression pathway. This includes, among others, COL1A1, COL1A2,
313 COL3A1, COL5A1, MMP8 and MMP9 (Supplementary Table S2). When comparing newly
314 diagnosed MM to healthy donor BM and that of MGUS, Interestingly, two proteins, Annexin
315 A2 and Galectin-1 are seen to emerge that are not present in earlier stages of the disease (Fig.
316 4B, Supplementary Table S2).

317

318 **MM cells present with an enrichment for ECM-related genes.**

319 We further validated the findings at the proteomic level by performing an analysis of the
320 corresponding mRNA gene expression in MM plasma cells.

321 Using the signature of ECM proteins found to be present in the normal ECM, and absent in
322 the MM tumor ECM, we performed GSEA to assess for enrichment of this gene signature in
323 healthy donors vs. MM patients. Enrichment of the corresponding ECM gene signature was

324 demonstrated in healthy donors compared to MM patients (Fig. 5A-B; FDR<0.25). It has
325 been shown that the majority of the tumor ECM is derived from the tumor cells in the main
326 part, with stromal contribution at different stages of metastasis (16). Our findings of an
327 altered ECM signature suggest that plasma cells may co-ordinate ECM remodeling in this
328 disease. The interaction between the altered ECM and other bone marrow micro-
329 environmental elements is likely to further augment the bone marrow milieu, creating a
330 permissive environment for MM progression.

331

332 **Annexin A2 and Galectin-1 and their prognostic relevance in MM.**

333 ANXA2 and LGALS1, two ECM-affiliated proteins, were identified in newly diagnosed MM
334 BM-ECMs, and not in healthy donor or MGUS BM-ECMs. We therefore analyzed the
335 expression of ANXA2 and LGALS1 in MM cell lines, using the Cancer Cell Line
336 Encyclopedia (CCLE); and found that both proteins were expressed in all MM cell lines (Fig.
337 6A and 7A). These observations were further corroborated by demonstrating the higher
338 expression of both ANXA2 and LGALS1 in BM MM- as compared to healthy donor-derived
339 plasma cells (GSE2658 and GSE6477; Fig. 6B and 7B) (22) (26).

340 Specifically, while ANXA2 levels were consistently higher in any given MGUS, smoldering-
341 MM, MM newly diagnosed or MM relapsed patient as compared to healthy donors, LGALS1
342 was significantly higher in MGUS and newly diagnosed MM patients as compared to healthy
343 individuals (Fig. 7B).

344 In order to further understand if these targets may be leading to a permissive tumor
345 microenvironment in MM, we analyzed the Mulligan dataset (27) for co-expression of these
346 genes in MM using the publically available Oncomine resource (www.oncomine.org); we
347 found that ANXA2 is one of the most highly co-expressed genes with LGALS1 in 264 MM
348 patients (Fig. 8A; correlation coefficient = 0.522).

349 We next interrogated the influence of both ANXA2 and LGALS1 in modulating survival in
350 MM patients. By examining GSE2658 (28), and found that patients expressing higher levels
351 of ANXA2 had a significantly reduced overall survival (OS) compared with those with lower
352 expression levels (Fig. 8B; Log-rank $p=4.9e-05$). Similarly, high levels of LGALS1 were also
353 associated with an inferior OS (Fig. 8C Log-rank $P = 0.05$)

354 **DISCUSSION**

355

356 In this study, we report the profiling of the ECM composition of normal bone marrow using
357 mass spectrometry. We have compared this profile to the composition of the ECM of patients
358 with MGUS, newly diagnosed, and relapsed multiple myeloma.

359 Our results demonstrate that significant remodeling of the bone marrow ECM is evident even
360 at the MGUS stage, with loss of collagens and fibronectin (COL4A1-A3, COL4A6,
361 COL5A2-3, COL6A2-3 COL10A1, COL11A2, COL16A1, COL27A1 and FN1). The
362 absence of these proteins was consistent throughout the spectrum of MM from newly
363 diagnosed to relapsed disease suggesting that the loss of these ECM components may
364 contribute to a permissive tumor microenvironment supportive of the development and
365 progression of MM. Indeed it has been shown that fibroblasts from patients with MGUS and
366 MM demonstrate altered ECM profiles in comparison to those of healthy donors, supporting
367 the hypothesis of early ECM remodeling (29).

368 Similarly, some collagens and matrix metallo-proteinases found in healthy donor bone
369 marrow are not detected at the MGUS stage but are seen to re-emerge in the disease
370 progression pathway indicating that they may be more supportive in aggressive phenotypes.
371 This includes, among others, COL1A1, COL1A2, COL3A1, COL5A1, MMP8 and MMP9.

372 Interestingly, two proteins, Annexin A2 (ANXA2) and Galectin-1 (LGALS1) were detected
373 in newly diagnosed MM but not in healthy donors or MGUS patients. These proteins were
374 confirmed as being expressed in MM cell lines at the mRNA level in CCLE datasets. We
375 hypothesized that these proteins may be required for myelomagenesis and further examined
376 their presence in MM patient bone marrow.

377 Our analysis of GEP profiles reveals that these proteins are highly expressed in MM bone
378 marrow plasma cells in comparison to healthy-donor-derived plasma cells. This may indicate
379 that these proteins are produced by the tumor cells within the bone marrow niche and are
380 specific to the malignant phenotype. If this is the case, then plasma cells themselves may
381 contribute to bone marrow ECM remodeling as has been shown in other tumors (16). This
382 may occur as a result of interactions between the remodeled ECM and other micro-
383 environmental elements as altered ECMs in cancer deregulate the behavior of stromal cells,
384 facilitate angiogenesis and promote a tumorigenic micro-environment (30). Altered ECM
385 composition and topography indirectly affects cancer cells by influencing the effect of
386 stromal cells, immune cells and fibroblasts which alters the tumor niche, this is also likely to
387 be the case in multiple myeloma given our findings, however further work is needed to
388 confirm this (30-32). Indeed, the galectins, of which LGALS1 is a member, are a family of
389 beta-galactoside-binding proteins implicated in modulating cell-cell and cell-matrix

390 interactions and recently Galectin-1 suppression has been shown to inhibit MM induced
391 angiogenesis and tumor growth *in-vivo* (33). Annexin A2 is a calcium dependent
392 phospholipid binding protein, which plays a role in cell growth and heightens osteoclast
393 formation and bone resorption. Osteoclasts are known to contribute to an immune
394 suppressive microenvironment in MM and are widely known to be associated with MM
395 pathogenesis (34). Also, ANXA2 has previously been shown to promote MM cell growth and
396 reduce apoptosis in MM cell lines (35). Identification of these targets, known to play a role in
397 MM biology, helps to provide a wider validation of the remodeling of the ECM signature
398 emerging using this novel strategy.

399 To further understand the implications of bone marrow remodeling in MM patients, we
400 examined if there might be a common expression pattern for these two proteins within the
401 MM bone marrow niche. Using data from Oncomine, we analyzed 264 MM patients and
402 found that ANXA2 is one of the most highly co-expressed genes with LGALS1 in these
403 patients. This leads us to hypothesize that the bone marrow remodeling seen in MM is likely
404 to be an organized process that occurs as a result of multiple ECM protein switches being
405 turned on and off within the bone marrow niche. Although both of these markers have
406 previously been identified as being important in MM, we have further validated them as
407 being part of an overall ECM remodeling process within the bone marrow.

408 The prognostic relevance of our findings was determined using GEP datasets, which provided
409 survival outcomes for MM patients. This demonstrated that patients expressing higher levels
410 of ANXA2 had a significantly reduced overall survival compared with those with lower
411 expression levels. Similarly, high levels of LGALS1 were also associated with a shorter
412 overall survival. This finding demonstrates that the bone marrow ECM plays an important
413 role in MM and suggests that ECM remodeling is an active process within the bone marrow
414 niche that has prognostic implications for MM patients. We can postulate that with the
415 development of i) technologies to characterize the proteome and the matrisome with greater
416 depth (including orthogonal peptide separation) and ii) methods to conduct quantitative
417 analyses, we will be able to identify many more proteins, some of which may have prognostic
418 values for MM patients. This previously under-evaluated area provides a potential resource
419 for the identification of novel targets in this disease which may lead the way to preserving the
420 normal ECM architecture and a less permissive niche.

421

422 **ACKNOWLEDGEMENTS**

423 This work was supported in part by NIH R01 CA181683-01A, R01 CA205954-01 and the
424 Leukemia and Lymphoma Society to IG, by the Health Research Board, Ireland, NSAFP of
425 which SG is a recipient, and in part by the Howard Hughes Medical Institute, of which ROH
426 is an Investigator.

427

428 **AUTHOR CONTRIBUTION**

429 SG, AN, SM, JS, ROH and IG **designed research.**

430 SG, AN, SM, MRR, MM, YM, AS, and JMA **performed research.**

431 AR, MG and AP **contributed clinical samples to this study.**

432 SG, AN, SM, ST, JP, JMA, AMR and KRC **analyzed data.**

433 SG, AN, SM, MOD, ROH and IG **wrote the paper.**

434

435 **CONFLICT-OF-INTEREST DISCLOSURES**

436 The authors have no conflicts of interest to declare

437

438 **REFERENCES**

- 439 1. Kyle RA, Rajkumar SV. Multiple myeloma. *N Engl J Med*. 2004;351(18):1860-73.
440 2. Ghobrial IM. Myeloma as a model for the process of metastasis: implications for
441 therapy. *Blood*. 2012;120(1):20-30.
442 3. Fowler JA, Mundy GR, Lwin ST, Edwards CM. Bone marrow stromal cells create a
443 permissive microenvironment for myeloma development: a new stromal role for Wnt
444 inhibitor Dkk1. *Cancer Res*. 2012;72(9):2183-9.
445 4. Manier S, Sacco A, Leleu X, Ghobrial IM, Roccaro AM. Bone marrow
446 microenvironment in multiple myeloma progression. *J Biomed Biotechnol*.
447 2012;2012:157496.
448 5. Kawano Y, Moschetta M, Manier S, Glavey S, Gorgun GT, Roccaro AM, et al.
449 Targeting the bone marrow microenvironment in multiple myeloma. *Immunol Rev*.
450 2015;263(1):160-72.
451 6. Kumar SK, Rajkumar SV, Dispenzieri A, Lacy MQ, Hayman SR, Buadi FK, et al.
452 Improved survival in multiple myeloma and the impact of novel therapies. *Blood*.
453 2008;111(5):2516-20.
454 7. Vincent T, Mechti N. Extracellular matrix in bone marrow can mediate drug
455 resistance in myeloma. *Leuk Lymphoma*. 2005;46(6):803-11.
456 8. Naba A, Clauser KR, Hoersch S, Liu H, Carr SA, Hynes RO. The matrisome: in silico
457 definition and in vivo characterization by proteomics of normal and tumor extracellular
458 matrices. *Mol Cell Proteomics*. 2012;11(4):M111 014647.
459 9. Hynes RO. The extracellular matrix: not just pretty fibrils. *Science*.
460 2009;326(5957):1216-9.
461 10. Schwartz MA. Integrins and extracellular matrix in mechanotransduction. *Cold*
462 *Spring Harb Perspect Biol*. 2010;2(12):a005066.
463 11. Naba A, Clauser KR, Whittaker CA, Carr SA, Tanabe KK, Hynes RO. Extracellular
464 matrix signatures of human primary metastatic colon cancers and their metastases to liver.
465 *BMC Cancer*. 2014;14:518.
466 12. Bergamaschi A, Tagliabue E, Sorlie T, Naume B, Triulzi T, Orlandi R, et al.
467 Extracellular matrix signature identifies breast cancer subgroups with different clinical
468 outcome. *J Pathol*. 2008;214(3):357-67.
469 13. Iozzo RV. Matrix proteoglycans: from molecular design to cellular function. *Annu*
470 *Rev Biochem*. 1998;67:609-52.
471 14. Ramaswamy S, Ross KN, Lander ES, Golub TR. A molecular signature of metastasis
472 in primary solid tumors. *Nat Genet*. 2003;33(1):49-54.
473 15. Hynes RO, Naba A. Overview of the matrisome--an inventory of extracellular matrix
474 constituents and functions. *Cold Spring Harb Perspect Biol*. 2012;4(1):a004903.
475 16. Naba A, Clauser KR, Lamar JM, Carr SA, Hynes RO. Extracellular matrix signatures
476 of human mammary carcinoma identify novel metastasis promoters. *Elife*. 2014;3:e01308.
477 17. Talmadge JE, Fidler IJ. AACR centennial series: the biology of cancer metastasis:
478 historical perspective. *Cancer Res*. 2010;70(14):5649-69.
479 18. Fidler IJ. The biology of cancer metastasis. *Semin Cancer Biol*. 2011;21(2):71.
480 19. Valastyan S, Weinberg RA. Tumor metastasis: molecular insights and evolving
481 paradigms. *Cell*. 2011;147(2):275-92.
482 20. Naba A, Clauser KR, Hynes RO. Enrichment of Extracellular Matrix Proteins from
483 Tissues and Digestion into Peptides for Mass Spectrometry Analysis. *J Vis Exp*.
484 2015(101):e53057.
485 21. Naba A, Clauser KR, Ding H, Whittaker CA, Carr SA, Hynes RO. The extracellular
486 matrix: Tools and insights for the "omics" era. *Matrix Biol*. 2016;49:10-24.

- 487 22. Chng WJ, Kumar S, Vanwier S, Ahmann G, Price-Troska T, Henderson K, et al.
488 Molecular dissection of hyperdiploid multiple myeloma by gene expression profiling. *Cancer*
489 *Res.* 2007;67(7):2982-9.
- 490 23. Barretina J, Caponigro G, Stransky N, Venkatesan K, Margolin AA, Kim S, et al. The
491 Cancer Cell Line Encyclopedia enables predictive modelling of anticancer drug sensitivity.
492 *Nature.* 2012;483(7391):603-7.
- 493 24. Zhan F, Huang Y, Colla S, Stewart JP, Hanamura I, Gupta S, et al. The molecular
494 classification of multiple myeloma. *Blood.* 2006;108(6):2020-8.
- 495 25. Subramanian A, Tamayo P, Mootha VK, Mukherjee S, Ebert BL, Gillette MA, et al.
496 Gene set enrichment analysis: a knowledge-based approach for interpreting genome-wide
497 expression profiles. *Proc Natl Acad Sci U S A.* 2005;102(43):15545-50.
- 498 26. Gutierrez NC, Sarasquete ME, Misiewicz-Krzeminska I, Delgado M, De Las Rivas J,
499 Ticona FV, et al. Deregulation of microRNA expression in the different genetic subtypes of
500 multiple myeloma and correlation with gene expression profiling. *Leukemia.* 2010;24(3):629-
501 37.
- 502 27. Mulligan G, Mitsiades C, Bryant B, Zhan F, Chng WJ, Roels S, et al. Gene
503 expression profiling and correlation with outcome in clinical trials of the proteasome
504 inhibitor bortezomib. *Blood.* 2007;109(8):3177-88.
- 505 28. Hanamura I, Huang Y, Zhan F, Barlogie B, Shaughnessy J. Prognostic value of cyclin
506 D2 mRNA expression in newly diagnosed multiple myeloma treated with high-dose
507 chemotherapy and tandem autologous stem cell transplantations. *Leukemia.*
508 2006;20(7):1288-90.
- 509 29. Slany A, Haudek-Prinz V, Meshcheryakova A, Bileck A, Lamm W, Zielinski C, et al.
510 Extracellular matrix remodeling by bone marrow fibroblast-like cells correlates with disease
511 progression in multiple myeloma. *J Proteome Res.* 2014;13(2):844-54.
- 512 30. Lu P, Weaver VM, Werb Z. The extracellular matrix: a dynamic niche in cancer
513 progression. *J Cell Biol.* 2012;196(4):395-406.
- 514 31. Bhowmick NA, Neilson EG, Moses HL. Stromal fibroblasts in cancer initiation and
515 progression. *Nature.* 2004;432(7015):332-7.
- 516 32. Orimo A, Gupta PB, Sgroi DC, Arenzana-Seisdedos F, Delaunay T, Naeem R, et al.
517 Stromal fibroblasts present in invasive human breast carcinomas promote tumor growth and
518 angiogenesis through elevated SDF-1/CXCL12 secretion. *Cell.* 2005;121(3):335-48.
- 519 33. Storti P, Marchica V, Airoidi I, Donofrio G, Fiorini E, Ferri V, et al. Galectin-1
520 suppression delineates a new strategy to inhibit myeloma-induced angiogenesis and tumoral
521 growth in vivo. *Leukemia.* 2016.
- 522 34. An G, Acharya C, Feng X, Wen K, Zhong M, Zhang L, et al. Osteoclasts promote
523 immune suppressive microenvironment in multiple myeloma: therapeutic implication. *Blood.*
524 2016;128(12):1590-603.
- 525 35. Seckinger A, Meissner T, Moreaux J, Depeweg D, Hillengass J, Hose K, et al.
526 Clinical and prognostic role of annexin A2 in multiple myeloma. *Blood.* 2012;120(5):1087-
527 94.

528

529

530

531

532

533

534 **FIGURE LEGENDS**

535

536 **Figure 1. Staining of fibrillar collagens using Masson's trichrome (blue) of mouse bone**
537 **marrow samples.**

538 **A.** Healthy murine bone marrow.

539 **B.** Multiple myeloma murine bone marrow.

540

541 **Figure 2. Staining of fibrillar collagens using Masson's trichrome (blue) of human bone**
542 **marrow samples.**

543 **A.** Healthy human bone marrow.

544 **B.** Multiple myeloma human bone marrow.

545

546 **Figure 3. Proteomic pipeline to characterize the ECM composition of normal and**
547 **diseased bone marrow samples.**

548 **A.** Experimental pipeline.

549 **B.** Western blot to control the efficiency of the decellularization of bone marrow samples.

550 Western blot shows the depletion of intracellular components (GAPDH, histones, Transferrin
551 receptor and vimentin) during the four-step decellularization process.

552 Coomassie-stained gel shows the pattern of migration of proteins from the ECM-enriched
553 samples.

554

555 **Figure 4. Comparison of the matrisome of normal and diseased bone marrow samples.**

556 **A.** Bar chart represents the number of proteins constituting the matrisome of normal, MGUS,
557 newly diagnosed MM, and relapsed MM bone marrow.

558 **B.** Venn diagram illustrated the overlap between the matrisome proteins detected in normal,
559 MGUS, newly diagnosed MM, and relapsed MM bone marrow (Supplementary Table S2).

560

561

562

563

564

565

566

567 **Figure 5. Gene set enrichment analysis of matrisome gene signature in MM patients.**

568 **A.** Gene set enrichment analysis (GSEA): demonstrating that (A) ECM proteins seen to be
569 depleted in the bone marrow matrix with disease progression were also significantly down
570 regulated at the gene level in normal donors (left) compared to MM patients (right).

571 **B.** Heatmap demonstrating enrichment profile of relevant ECM genes in healthy donors vs.
572 MM patients.

573 **Figure 6: Gene expression of ANXA2 in MM cell lines.**

574 **A.** Analysis of CCLE MM cell lines (red bars) demonstrating the expression ANXA2 in MM
575 cell lines at the mRNA level.

576 **B.** ANXA2 is significantly overexpressed at the mRNA level in MGUS, smoldering MM
577 (SMM), newly diagnosed MM (MM, ndx) and relapsed MM (MM relapse) in comparison to
578 normal donors (ND). Dataset reference: Cancer Res. 2007 Apr 1;67(7):2982-9. (GSE6477)

579

580 **Figure 7: Gene expression of LGALS1 in MM cell lines.**

581 **A.** LGALS1 is also significantly overexpressed at the mRNA level in newly diagnosed MM
582 patients compared to normal donors in CCLE dataset.

583 **B.** LGALS1 is significantly overexpressed at the mRNA level in MGUS, smoldering MM
584 (SMM), newly diagnosed MM (MM, ndx) and relapsed MM (MM relapse) in comparison to
585 normal donors (ND). Dataset reference: Cancer Res. 2007 Apr 1;67(7):2982-9. (GSE6477)

586

587 **Figure 8. Expression of ECM proteins in MM patients and impact on overall survival.**

588 **A.** Co-expression of LGALS1 and ANXA2 in MM patients – data sourced from Oncomine
589 (www.oncomine.org) Mulligan MM gene expression Blood. 2007 Apr 15;109(8):3177-88.
590 Epub 2006 Dec 21.

591 **B.** Kaplan-Meier survival proportions analysis of patient outcome data from the GSE2658
592 MM GEP dataset demonstrating high levels of ANXA2 expression associated with inferior
593 overall survival. Log-rank $P = 4.9e-05$

594 **C.** Kaplan-Meier survival proportions analysis of patient outcome data from the GSE2658
595 MM GEP dataset demonstrating high levels of LGALS1 expression associated with inferior
596 overall survival. Log-rank $P = 0.051$.

597

598

599

600 **Supplementary Table S1. Bone marrow matrisome.** Matrisome of the bone marrow from
601 healthy donors (A), MGUS patients (B), newly diagnosed multiple myeloma patients (C), and

602 relapsed multiple myeloma patients (D). * indicates ECM or ECM-associated proteins not
603 detected before in any human tissue matrisome.

604

605 **Supplementary Table S2. Comparison of the matrisome of normal, MGUS, newly**
606 **diagnosed MM, and relapsed MM bone marrow**

607 **Supplementary Table S3. Proteomic data**

608 **A.** Complete proteomic dataset. Proteins are sorted by matrisome categories and then by
609 Entrez Gene Symbol.

610 **B-E.** The total precursor-ion intensity, number of spectra and unique peptides were calculated
611 for each protein and in each sample. Proteins are sorted by number of observations (column
612 D), then matrisome categories (column B) and gene symbols (column C). Proteins detected in
613 at least 3 patients and with at least 3 peptides in one of the samples compose the matrisome
614 of each of the four bone marrow sample types (bold).

615 **B.** All ECM and ECM-associated proteins detected in normal bone marrow samples.

616 **C.** All ECM and ECM-associated proteins detected in bone marrow samples from MGUS
617 samples.

618 **D.** All ECM and ECM-associated proteins detected in bone marrow samples from newly
619 diagnosed multiple myeloma patients.

620 **E.** All ECM and ECM-associated proteins detected in bone marrow samples from relapsed
621 multiple myeloma patients.

622 **F.** Name of raw mass spectrometry files.

623

624 **Supplementary Figure 1: Proteomic metrics.**

625 Pie charts represent relative amount of core matrisome (blue), matrisome-associated (orange)
626 and other (grey) proteins in terms of peptide abundance, and numbers of spectra, unique
627 peptides and proteins.

628 **A.** Metrics for representative normal bone marrow sample.

629 **B.** Metrics for representative MGUS sample.

630 **C.** Metrics for representative newly diagnosed multiple myeloma sample.

631 **D.** Metrics for representative relapsed multiple myeloma sample.

632

633 **Supplementary Figure 2: ECM peptide abundance**

634 Bar charts represent the peptide abundance for ECM vs non-ECM proteins (**A**) and for core
635 matrisome and matrisome-associated proteins (**B**) in each sample analyzed.

636

Proteomic characterization of human multiple myeloma bone marrow extracellular matrix

Siobhan V. Glavey^{1,7*}, Alexandra Naba^{2,¶,*}, Salomon Manier^{1*}, Karl Clauser³, Sabrin Tahri¹, Jihye Park¹, Michaela R. Reagan¹, Michele Moschetta¹, Yuji Mishima¹, Manuela Gambella⁴, Alberto Rocci⁵, Antonio Sacco^{1,6}, Michael E O'Dwyer⁷, John M. Asara⁸, Antonio Palumbo⁴, Aldo M. Roccaro^{1,6, #}, Richard O. Hynes^{2,9,#}, Irene M. Ghobrial^{1#}

¹Dana Farber Cancer Institute, Harvard Medical School, Boston, MA, USA; ²Koch Institute for Integrative Cancer Research, Massachusetts Institute of Technology, Cambridge, MA, USA;

³Proteomics Platform, Broad Institute, Cambridge, MA, USA; ⁴University of Torino, Azienda Ospedaliero-Universitaria Città della Salute e della Scienza di Torino, Torino, Italy; ⁵Manchester Royal Infirmary and Central Manchester University Hospital NHS Foundation, University of Manchester, Manchester, United Kingdom; ⁶SST Spedali Civili, Dept. Medical Oncology, CREA Laboratory, Brescia, Italy; ⁷Department of Hematology, National University of Ireland, Galway, Ireland; ⁸Beth Israel Deaconess Medical Center, Harvard Medical School, Boston, MA, USA;

⁹Howard Hughes Medical Institute, Massachusetts Institute of Technology, Cambridge, MA, USA.

[¶]AN Present address: Department of Physiology and Biophysics, University of Illinois at Chicago, Chicago, IL 60612, USA

* S.G, A.N and S.M. contributed equally to this study.

AMR, ROH, IMG: co-last Authors

Running title: Matrisome of human multiple myeloma

Corresponding authors:

Irene M. Ghobrial, MD

Dana-Farber Cancer Institute, Boston, MA, USA

Tel: +1 617.632.6777

E-mail: Irene_ghobrial@dfci.harvard.edu

Richard O Hynes, PhD

Koch Institute for Integrative Cancer Research at MIT, Cambridge, MA, USA

Tel: +1 617.253.6422

E-mail: rohynes@mit.edu

ABSTRACT

The extracellular matrix (ECM) is a major component of the tumor microenvironment, contributing to the regulation of cell survival, proliferation, differentiation and metastasis. In multiple myeloma (MM), interactions between MM cells and the bone marrow (BM) microenvironment, including the BM ECM, are critical to the pathogenesis of the disease and the development of drug resistance. Nevertheless, composition of the ECM in MM and its role in supporting MM pathogenesis has not been reported. We have applied a novel proteomic-based strategy and defined the BM ECM composition in patients with monoclonal gammopathy of undetermined significance (MGUS), newly diagnosed and relapsed MM compared to healthy donor-derived BM ECM. In this study, we show that the tumor ECM is remodeled at the mRNA and protein level in MGUS and MM to allow development of a permissive microenvironment. We further demonstrate that two ECM-affiliated proteins, ANXA2 and LGALS1, are more abundant in MM and high expression is associated with a decreased overall survival. This study points to the importance of ECM remodeling in MM and provides a novel proteomic pipeline for interrogating the role of the ECM in cancers with BM tropism.

Keywords: Multiple Myeloma, Extracellular Matrix, Proteomics

INTRODUCTION

Multiple myeloma (MM) is a plasma cell malignancy and accounts for approximately 10% of all hematological cancers (1). MM provides a model for the study of cancer cell metastasis as MM cells are known to traffic to distant bone marrow (BM) niches via hijacking the normal processes of cellular metastasis (2). Progression of the disease is mediated by intrinsic factors of the clonal cells along with factors that mediate a permissive tumor microenvironment (3). The MM tumor niche comprises the components of the BM microenvironment - cellular (stromal cells, osteoblasts, osteoclasts, endothelial cells and immune cells) and non-cellular (ECM) (4, 5). Despite advances in therapies in recent years, MM remains an incurable disease with a median survival of approximately 5-7 years for newly diagnosed patients (6). Identification of the molecular mechanisms leading to MM has the potential to lead to the development of novel prognostic tests and therapies for MM patients (7)(8).

The extracellular matrix (ECM) is a complex meshwork of proteins that serves as a scaffold for cells. In addition, it actively participates in cell functions such as proliferation, migration and survival via cell-to-matrix interactions (9, 10). The ECM is also rich in growth factors and cytokines thus supporting cell biology (9); therefore it follows that alterations in the ECM may be expected to occur in disease states such as inflammation and cancer. This is indeed the case in several tumor types where ECM alterations have been associated with changes in metastatic potential of tumor cells *in vivo* and in clinical outcomes (11, 12). The role of the ECM as a metabolic regulator of cell function also has implications for malignant processes (13) and molecular signals of metastasis have implicated ECM components and their receptors in tumor progression (14). In the past, attempts to systematically characterize the ECM were challenged by the vast diversity and number of ECM proteins and also by their biochemical nature. A new perspective on analysis of the ECM, on a relatively high throughput scale, came with the definition and *in-vivo* characterization of the “matrisome” (8). The term “matrisome”, initially used by Martin and collaborators in 1984 was updated and refined by Naba et al in 2012. This study revealed tissue specific signatures of ECM proteins and importantly provided a method to determine the origin (tumor cell or stroma) of individual matrix proteins. The “matrisome” itself is defined as the components constituting the ECM “core matrisome” and all associated components “matrisome associated”. This method has yielded important insights into the composition of several solid tumor matrices

along with potential novel therapeutic and prognostic targets (11, 15). ECM alterations that influence cellular metastasis have implications not only for solid tumors but also for hematological malignancies, where the process of cell migration from the primary niche is largely dependent on the tumor microenvironment (16-18).

In this study we apply a mass-spectrometry-based proteomic pipeline to study the tumor ECM from the bone marrow of MM patients. We characterize the unique extracellular matrices of patients with the pre-myeloma condition monoclonal gammopathy of undetermined significance (MGUS), newly diagnosed and relapsed MM patients and compare these ECM signatures to that of healthy human donor bone marrow. Our results demonstrate ECM remodeling with disease progression, as early at the MGUS stage. We further identify ANXA2 and LGALS1, two ECM-associated proteins as markers of the MM ECM and show the prognostic value of their expression for multiple-myeloma-patient overall survival.

MATERIALS AND METHODS

Human bone marrow aspirates. Informed consent was obtained from all patients in accordance with the Declaration of Helsinki. These studies were approved by the Dana-Farber Cancer Institute Institutional Review Board and the University of Torino, Italy. Whole bone marrow (BM) was obtained from healthy human donors (n=10), MGUS patients (n=3), newly diagnosed MM patients who had not yet received treatment (n=7) and patients with relapsed MM (n=6). Fresh BM samples (20ml/patient) were filtered and underwent red cell lysis, followed by centrifugation at 2500rpm for 10 minutes (see Supplementary Methods for full protocol). The isolated pellet was then processed through the sequential extraction methods outlined below.

ECM protein enrichment and SDS gradient gel separation. ECM protein enrichment from of whole BM samples was achieved by sequentially depleting intracellular proteins as previously described (8, 19). In brief, whole BM samples were homogenized and subjected to incubations in different buffers to remove (1) cytosolic proteins, (2) nuclear proteins, (3) membrane proteins and (4) cytoskeletal proteins, leaving a final insoluble fraction enriched for ECM proteins.

Immunoblotting. For validation of the extraction process, the different fractions were separated on SDS-polyacrylamide gradient gels, transferred to nitrocellulose membranes and probed with relevant subcellular compartmental antibodies to confirm elimination of intracellular proteins and enrichment of ECM proteins. The antibodies used for immunoblotting included anti-GAPDH, anti-Histone (Cell Signaling Technology, Danvers, MA), anti-transferrin (Invitrogen, Camarillo, CA), anti-vimentin (Cell Signaling Technology, Danvers, MA), anti-fibronectin (Abcam, Cambridge, MA), anti-actin (Santa Cruz Biotechnology, Dallas, TX) or anti- α -tubulin (Cell Signaling Technology, Danvers, MA).

Protein digestion in peptides. The ECM-enriched protein fractions obtained after decellularization were solubilized and reduced in a solution of 8M urea in 100mM ammonium bicarbonate containing 10mM dithiothreitol at 37°C for 30 minutes. The solubilized ECM proteins were then separated on 4-20% SDS-polyacrylamide gradient gels. Gels were stained with Gel Code Blue (Thermo Scientific) and washed in dH₂O. Gels were

then cut into 2 or 3 pieces using a clean scalpel and gel pieces were transferred into clean microcentrifuge tubes. Gel bands were wash twice with 200mL of 50% acetonitrile for 15 min. Protein gel samples were reduced with 10mM DTT, alkylated with 55mM iodoacetamide and digested overnight with 100ng of sequencing grade TPCK modified trypsin (Promega) at pH=8.3. Samples were acidified with 0.5% trifluoroacetic acid and desalted using C18 zip tips (Millipore) and concentrated to 10uL.

Liquid chromatography and Tandem Mass Spectrometry. 2 to 4uL of peptides were analyzed by microcapillary liquid chromatography (C18) tandem mass spectrometry (LC-MS/MS) using an EASY-nLCII nanoflow HPLC (Thermo Fisher Scientific) coupled to a hybrid Orbitrap Elite high-resolution mass spectrometer (Thermo Fisher Scientific) in Top 6 data-dependent acquisition positive ion mode at a flow rate of 300 nL/min.

Protein and peptide identification. The LC-MS/MS datasets were analyzed with the Spectrum Mill software package, v 5.0 pre-release (Agilent Technologies, Santa Clara, CA). MS/MS spectra were searched against UniProt databases containing reference proteome sequences (including isoforms and excluding fragments) downloaded from the UniProt web site on October 17, 2014. Redundant sequences were removed, and a set of common laboratory contaminant proteins (150 sequences) was appended. The human database comprised 59,079 entries. Search criteria, described in the Supplementary Methods, yielded target-decoy-based false-discovery rate estimates for each patient's dataset of <0.8% at the peptide-spectrum match level and <1.3 % at the distinct peptide level. Across all datasets together the peptide-level FDR was 1.9%. Peptide-spectrum matches from all datasets together were assembled into proteins, and each protein was annotated as ECM-derived or not, as previously described (8, 20).

The raw mass spectrometric data have been deposited to the ProteomeXchange Consortium.

Analysis of gene expression profiling and survival analysis. Publicly available gene expression profiles (GEP) were analyzed to evaluate the expression level of ANXA2 and LGALS1 in MM patient samples and cell lines (GSE6477)(21). We used the Cancer Cell Line Encyclopedia (CCLE) database (<http://www.broadinstitute.org/ccle/home>)(22) to determine the expression level of ANXA2 and LGALS1 across over 1,000 cell lines, expressed by Robust Multi-array Average (RMA) values. We further studied GEP to assess the differential expression of ANXA2 and LGALS1 in MM vs. normal plasma cells –

GSE6477. Gene levels were expressed by normalized expression values and 2-tailed t test were calculated to compare the 2 groups. Finally, we analyzed a large GEP - GSE2658 (23) – that enrolled 350 patients at diagnosis of MM. A Kaplan-Meier analysis was performed to compare overall survival (OS) of patients with low vs. high expression level of ANXA2 or LGALS1 based on the median expression of the cohort.

Gene set enrichment analysis (GSEA). We performed gene set enrichment analysis (GSEA)(24) to determine whether the identified ECM gene sets followed the same pattern at the mRNA level in MM patients compared to healthy donors. GSEA was performed following the developer’s protocol (<http://www.broad.mit.edu/gsea/>) using the GSEA6477 dataset (21).

RESULTS

ECM protein enrichment from normal and diseased whole bone marrow samples.

We have examined murine and human BM, using Masson's trichrome to stain fibrillar collagens, as an assessment of ECM content (Fig. 1 and 2). We identified ECM within healthy murine BM niches and observed that the normal architecture of the ECM became disorganized in MM murine bone marrow but was still clearly present (Fig. 1A and B). Similarly, ECM was also identifiable within the BM of MM patients (Fig. 2 A and B), where morphology most resembled that seen in the MM murine BM. In order to isolate and characterize this ECM, we developed a protocol based on the previous decellularization method devised by Naba et al (8) specifically tailored to enrich for insoluble ECM proteins from the liquid marrow (Fig. 3A). Antibody markers, including anti-GAPDH, -histone, -transferrin receptor, and -vimentin were used for the cytosolic, nuclear, membrane and cytoskeletal compartments in order to confirm depletion of intracellular components at each step (Fig. 3B, left panel). In addition, we used an anti-fibronectin antibody to monitor the behavior of one exemplary ECM protein during the decellularization of bone marrow samples. Although we observed a portion of fibronectin to be partially depleted at each step, it was present in the final fraction (Fig. 3B, left panel). The protein fraction that remains insoluble after decellularization was then separated using gel electrophoresis, gels were stained using Coomassie blue stain (Fig. 3B, right panel). Gel bands were further cut from the gels and proteins were subjected to in-gel protein digestion to generate peptides to be separated by liquid chromatography and analyzed by mass spectrometry.

Proteomic characterization of healthy human donor, MGUS and MM ECM.

We aimed to define the proteomic signature of BM ECMs obtained from patients with MGUS and MM, as compared to healthy donors-derived BM ECMs. Complete data acquired on independent samples from healthy donors, MGUS patients and MM patients is shown in Supplementary Table S3. Peptide abundance, spectral count, number of unique peptides and number of proteins identified within the whole bone marrow were measured for both healthy donors and patients with MGUS or MM, either at first diagnosis or at relapse (Supplementary Fig. S1). In a representative healthy donor-derived sample, 24% of total spectral count signals were core matrisome or matrisome associated with 43% of the total precursor-ion intensity corresponding to proteins defined as ECM (Fig. S1A). A similar pattern was demonstrated for MGUS, newly diagnosed and relapsed MM BM ECMs (Fig. S1B-D. and

Supplementary Table S3B-E). In previous studies conducted on solid tumors (melanoma or mammary tumor xenografts, and human metastatic colorectal carcinomas), we have reported that the majority, typically (>75%) of the total precursor-ion intensities, correspond to matrisome proteins (8, 11, 15). This may reveal that the bone marrow ECM is more soluble and more readily extractable during the decellularization process than the ECM of normal tissues and solid tumors. In addition, it is worth noting that the inter-patient variability was greater than what we previously observed in solid tumor¹¹. Starting with 20 ml of bone marrow aspirate for each donor or patient, we observed that the proportion of the total precursor-ion intensities corresponding to matrisome proteins ranged from 10% to nearly 50%, (see Supplementary Fig. S2 and Supplementary Table S3A).

Characterization of the matrisome from healthy donor bone marrow.

We defined the matrisome of healthy-donor-derived BM as the ensemble of proteins detected in at least three independent biological replicates (i.e. patients) and by at least three peptides in one of the replicates. According to this definition the BM ECM from 10 independent healthy donors was composed of 62 proteins (Supplementary Table S1A). We previously proposed to classify proteins as part of the core matrisome, which comprises ECM glycoproteins, collagens, and proteoglycans, or being matrisome-associated proteins (ECM-affiliated proteins, ECM regulators, and ECM-associated secreted factors) (8, 20). The human bone marrow matrisome comprises 30 core matrisome proteins and 32 matrisome-associated proteins (Supplementary Table S1A, Supplementary Table S3B). The interrogation of the MatrisomeDB database (20) further revealed the identification of 11 proteins that have not been previously detected in any of the human tissues included in the database (Supplementary Table S1A). As human BM has not been previously subjected to this type of method, these proteins may be specific to this tissue.

Characterization of the matrisome from MGUS and MM patients.

We next sought to define the proteomic signature for BM ECMs derived from MGUS patients, using the same criteria outlined above, and found 11 proteins, two of which were core matrisome proteins, namely Bone Marrow Proteoglycan 2 (PRG2) and Bone Marrow proteoglycan 3 (PRG3) (Supplementary Table S1B). Nine of the proteins identified in the MGUS patient bone marrows were matrisome associated, including the ECM-affiliated protein ficolin 1 (FCN1), the ECM-remodeling enzymes CTSG, Serpins, and the secreted factors HRNR, S100A8 and S100A9 (Supplementary Table S1B).

Analysis of the ECM signature of MM bone marrow identified 32 proteins (Supplementary Table S1C). Ten of these proteins were core matrisome proteins, with 22 being matrisome associated. Interestingly two proteins were identified as matrisome associated, Annexin A2 (ANXA2) and Galectin-1 (LGALS1), which were not identified at a significant level in healthy donor or MGUS bone marrow. The ECM of patients with relapsed MM comprised of 25 proteins, 10 of which are core matrisome proteins and 15 of which are matrisome associated (Supplementary Table S1D).

The analysis of the ECM identified signatures of MGUS and progressive MM.

By comparing the matrisomes of healthy donor bone marrow, MGUS and progressive stages of MM, we identified 11 proteins expressed by all four groups (Fig. 4A-B). Examples of these proteins are cathepsin-G (CTSG) and neutrophil elastase (ELANE). We further remarked that the normal-bone-marrow matrisome contained more proteins than diseased bone marrow samples. Because the proteomic pipeline employed analyzed only proteins that remained insoluble after decellularization, one hypothesis is that the ECM proteins in MGUS or MM bone marrow samples are more soluble. In agreement with this hypothesis, we observed the loss of several collagens and other fibrillar ECM glycoproteins such as fibronectin in MGUS and MM samples (Supplementary Table S2, Supplementary Table S3B-E). We also observed that some collagens and matrix metallo-proteinases (MMPs) found in healthy donor bone marrow and not detected at the MGUS stage are detected later in the disease progression pathway. This includes, among others, COL1A1, COL1A2, COL3A1, COL5A1, MMP8 and MMP9 (Supplementary Table S2). When comparing newly diagnosed MM to healthy donor BM and that of MGUS, Interestingly, two proteins, Annexin A2 and Galectin-1 are seen to emerge that are not present in earlier stages of the disease (Fig. 4B, Supplementary Table S2).

MM cells present with an enrichment for ECM-related genes.

We further validated the findings at the proteomic level by performing an analysis of the corresponding mRNA gene expression in MM plasma cells.

Using the signature of ECM proteins found to be present in the normal ECM, and absent in the MM tumor ECM, we performed GSEA to assess for enrichment of this gene signature in healthy donors vs. MM patients. Enrichment of the corresponding ECM gene signature was demonstrated in healthy donors compared to MM patients (Fig. 5A-B; FDR<0.25). It has been shown that the majority of the tumor ECM is derived from the tumor cells in the main

part, with stromal contribution at different stages of metastasis (15). Therefore, our findings suggest the ability of tumor cells to contribute to micro-environmental remodeling.

Annexin A2 and Galectin-1 and their prognostic relevance in MM.

ANXA2 and LGALS1, two ECM-affiliated proteins, were identified in newly diagnosed MM BM-ECMs, and not in healthy donor or MGUS BM-ECMs. We therefore analyzed the expression of ANXA2 and LGALS1 in MM cell lines, using the Cancer Cell Line Encyclopedia (CCLE); and found that both proteins were expressed in all MM cell lines (Fig. 6A and 7A). These observations were further corroborated by demonstrating the higher expression of both ANXA2 and LGALS1 in BM MM- as compared to healthy donor-derived plasma cells (GSE2658 and GSE6477; Fig. 6B and 7B) (21) (25).

Specifically, while ANXA2 levels were consistently higher in any given MGUS, smoldering-MM, MM newly diagnosed or MM relapsed patient as compared to healthy donors, LGALS1 was significantly higher in MGUS and newly diagnosed MM patients as compared to healthy individuals (Fig. 7B).

In order to further understand if these targets may be leading to a permissive tumor microenvironment in MM, we analyzed the Mulligan dataset (26) for co-expression of these genes in MM using the publically available Oncomine resource (www.oncomine.org); we found that ANXA2 is one of the most highly co-expressed genes with LGALS1 in 264 MM patients (Fig. 8A; correlation coefficient = 0.522).

We next interrogated the influence of both ANXA2 and LGALS1 in modulating survival in MM patients. By examining GSE2658 (27), and found that patients expressing higher levels of ANXA2 had a significantly reduced overall survival (OS) compared with those with lower expression levels (Fig. 8B; Log-rank $p=4.9e-05$). Similarly, high levels of LGALS1 were also associated with an inferior OS (Fig. 8C Log-rank $P = 0.05$)

DISCUSSION

In this study, we report the profiling of the ECM composition of normal bone marrow using mass spectrometry. We have compared this profile to the composition of the ECM of patients with MGUS, newly diagnosed, and relapsed multiple myeloma.

Our results demonstrate that significant remodeling of the bone marrow ECM is evident even at the MGUS stage, with loss of collagens and fibronectin (COL4A1-A3, COL4A6, COL5A2-3, COL6A2-3 COL10A1, COL11A2, COL16A1, COL27A1 and FN1). The absence of these proteins was consistent throughout the spectrum of MM from newly diagnosed to relapsed disease suggesting that the loss of these ECM components may contribute to a permissive tumor microenvironment supportive of the development and progression of MM. Indeed it has been shown that fibroblasts from patients with MGUS and MM demonstrate altered ECM profiles in comparison to those of healthy donors, supporting the hypothesis of early ECM remodeling (28).

Similarly, some collagens and matrix metallo-proteinases found in healthy donor bone marrow are not detected at the MGUS stage but are seen to re-emerge in the disease progression pathway indicating that they may be more supportive in aggressive phenotypes. This includes, among others, COL1A1, COL1A2, COL3A1, COL5A1, MMP8 and MMP9.

Interestingly, two proteins, Annexin A2 (ANXA2) and Galectin-1 (LGALS1) were detected in newly diagnosed MM but not in healthy donors or MGUS patients. These proteins were confirmed to be expressed in MM cell lines at the mRNA level in CCLE datasets. We hypothesized that these proteins may be required for myelomagenesis and further examined their presence in MM patient bone marrow.

Our analysis of GEP profiles reveals that these proteins are highly expressed in MM bone marrow plasma cells in comparison to healthy-donor-derived plasma cells. This may indicate that these proteins are produced by the tumor cells within the bone marrow niche and are specific to the malignant phenotype. If this is the case, then plasma cells themselves may contribute to bone marrow ECM remodeling as has been shown in other tumors (15).

Indeed, the galectins, of which LGALS1 is a member, are a family of beta-galactoside-binding proteins implicated in modulating cell-cell and cell-matrix interactions and recently Galectin-1 suppression has been shown to inhibit MM induced angiogenesis and tumor growth *in-vivo* (29). Annexin A2 is a calcium dependent phospholipid binding protein, which plays a role in cell growth and heightens osteoclast formation and bone resorption. Osteoclasts are known to contribute to an immune suppressive microenvironment in MM and

are widely known to be associated with MM pathogenesis (30). Also, ANXA2 has previously been shown to promote MM cell growth and reduce apoptosis in MM cell lines (31). Identification of these targets, known to play a role in MM biology, helps to provide a wider validation of the remodeling of the ECM signature emerging using this novel strategy.

To further understand the implications of bone marrow remodeling in MM patients, we examined if there might be a common expression pattern for these two proteins within the MM bone marrow niche. Using data from Oncomine, we analyzed 264 MM patients and found that ANXA2 is one of the most highly co-expressed genes with LGALS1 in these patients. This leads us to hypothesize that the bone marrow remodeling seen in MM is likely to be an organized process that occurs as a result of multiple ECM protein switches being turned on and off within the bone marrow niche. Although both of these markers have previously been identified as being important in MM, we have further validated them as being part of an overall ECM remodeling process within the bone marrow.

The prognostic relevance of our findings was determined using GEP datasets, which provided survival outcomes for MM patients. This demonstrated that patients expressing higher levels of ANXA2 had a significantly reduced overall survival compared with those with lower expression levels. Similarly, high levels of LGALS1 were also associated with a shorter overall survival. This finding demonstrates that the bone marrow ECM plays an important role in MM and suggests that ECM remodeling is an active process within the bone marrow niche that has prognostic implications for MM patients. We can postulate that with the development of i) technologies to characterize the proteome and the matrisome with greater depth (including orthogonal peptide separation) and ii) methods to conduct quantitative analyses, we will be able to identify many more proteins, some of which may have prognostic values for MM patients. This previously under-evaluated area provides a potential resource for the identification of novel targets in this disease which may lead the way to preserving the normal ECM architecture and a less permissive niche.

ACKNOWLEDGEMENTS

This work was supported in part by NIH R01 CA181683-01A, R01 CA205954-01 and the Leukemia and Lymphoma Society to IG, by the Health Research Board, Ireland, NSAFP of which SG is a recipient, and in part by the Howard Hughes Medical Institute, of which ROH is an Investigator.

AUTHOR CONTRIBUTION

SG, AN, SM, JS, ROH and IG **designed research.**

SG, AN, SM, MRR, MM, YM, AS, and JMA **performed research.**

AR, MG and AP **contributed clinical samples to this study.**

SG, AN, SM, ST, JP, JMA, AMR and KRC **analyzed data.**

SG, AN, SM, MOD, ROH and IG **wrote the paper.**

CONFLICT-OF-INTEREST DISCLOSURES

The authors have no conflicts of interest to declare

REFERENCES

1. Kyle RA, Rajkumar SV. Multiple myeloma. *N Engl J Med*. 2004;351(18):1860-73.
2. Ghobrial IM. Myeloma as a model for the process of metastasis: implications for therapy. *Blood*. 2012;120(1):20-30.
3. Fowler JA, Mundy GR, Lwin ST, Edwards CM. Bone marrow stromal cells create a permissive microenvironment for myeloma development: a new stromal role for Wnt inhibitor Dkk1. *Cancer Res*. 2012;72(9):2183-9.
4. Manier S, Sacco A, Leleu X, Ghobrial IM, Roccaro AM. Bone marrow microenvironment in multiple myeloma progression. *J Biomed Biotechnol*. 2012;2012:157496.
5. Kawano Y, Moschetta M, Manier S, Glavey S, Gorgun GT, Roccaro AM, et al. Targeting the bone marrow microenvironment in multiple myeloma. *Immunol Rev*. 2015;263(1):160-72.
6. Kumar SK, Rajkumar SV, Dispenzieri A, Lacy MQ, Hayman SR, Buadi FK, et al. Improved survival in multiple myeloma and the impact of novel therapies. *Blood*. 2008;111(5):2516-20.
7. Vincent T, Mechti N. Extracellular matrix in bone marrow can mediate drug resistance in myeloma. *Leuk Lymphoma*. 2005;46(6):803-11.
8. Naba A, Clauser KR, Hoersch S, Liu H, Carr SA, Hynes RO. The matrisome: in silico definition and in vivo characterization by proteomics of normal and tumor extracellular matrices. *Mol Cell Proteomics*. 2012;11(4):M111 014647.
9. Hynes RO. The extracellular matrix: not just pretty fibrils. *Science*. 2009;326(5957):1216-9.
10. Schwartz MA. Integrins and extracellular matrix in mechanotransduction. *Cold Spring Harb Perspect Biol*. 2010;2(12):a005066.
11. Naba A, Clauser KR, Whittaker CA, Carr SA, Tanabe KK, Hynes RO. Extracellular matrix signatures of human primary metastatic colon cancers and their metastases to liver. *BMC Cancer*. 2014;14:518.
12. Bergamaschi A, Tagliabue E, Sorlie T, Naume B, Triulzi T, Orlandi R, et al. Extracellular matrix signature identifies breast cancer subgroups with different clinical outcome. *J Pathol*. 2008;214(3):357-67.
13. Iozzo RV. Matrix proteoglycans: from molecular design to cellular function. *Annu Rev Biochem*. 1998;67:609-52.
14. Ramaswamy S, Ross KN, Lander ES, Golub TR. A molecular signature of metastasis in primary solid tumors. *Nat Genet*. 2003;33(1):49-54.
15. Naba A, Clauser KR, Lamar JM, Carr SA, Hynes RO. Extracellular matrix signatures of human mammary carcinoma identify novel metastasis promoters. *Elife*. 2014;3:e01308.
16. Talmadge JE, Fidler IJ. AACR centennial series: the biology of cancer metastasis: historical perspective. *Cancer Res*. 2010;70(14):5649-69.
17. Fidler IJ. The biology of cancer metastasis. *Semin Cancer Biol*. 2011;21(2):71.
18. Valastyan S, Weinberg RA. Tumor metastasis: molecular insights and evolving paradigms. *Cell*. 2011;147(2):275-92.
19. Naba A, Clauser KR, Hynes RO. Enrichment of Extracellular Matrix Proteins from Tissues and Digestion into Peptides for Mass Spectrometry Analysis. *J Vis Exp*. 2015(101):e53057.
20. Naba A, Clauser KR, Ding H, Whittaker CA, Carr SA, Hynes RO. The extracellular matrix: Tools and insights for the "omics" era. *Matrix Biol*. 2016;49:10-24.
21. Chng WJ, Kumar S, Vanwier S, Ahmann G, Price-Troska T, Henderson K, et al. Molecular dissection of hyperdiploid multiple myeloma by gene expression profiling. *Cancer Res*. 2007;67(7):2982-9.

22. Barretina J, Caponigro G, Stransky N, Venkatesan K, Margolin AA, Kim S, et al. The Cancer Cell Line Encyclopedia enables predictive modelling of anticancer drug sensitivity. *Nature*. 2012;483(7391):603-7.
23. Zhan F, Huang Y, Colla S, Stewart JP, Hanamura I, Gupta S, et al. The molecular classification of multiple myeloma. *Blood*. 2006;108(6):2020-8.
24. Subramanian A, Tamayo P, Mootha VK, Mukherjee S, Ebert BL, Gillette MA, et al. Gene set enrichment analysis: a knowledge-based approach for interpreting genome-wide expression profiles. *Proc Natl Acad Sci U S A*. 2005;102(43):15545-50.
25. Gutierrez NC, Sarasquete ME, Misiewicz-Krzeminska I, Delgado M, De Las Rivas J, Ticona FV, et al. Deregulation of microRNA expression in the different genetic subtypes of multiple myeloma and correlation with gene expression profiling. *Leukemia*. 2010;24(3):629-37.
26. Mulligan G, Mitsiades C, Bryant B, Zhan F, Chng WJ, Roels S, et al. Gene expression profiling and correlation with outcome in clinical trials of the proteasome inhibitor bortezomib. *Blood*. 2007;109(8):3177-88.
27. Hanamura I, Huang Y, Zhan F, Barlogie B, Shaughnessy J. Prognostic value of cyclin D2 mRNA expression in newly diagnosed multiple myeloma treated with high-dose chemotherapy and tandem autologous stem cell transplantations. *Leukemia*. 2006;20(7):1288-90.
28. Slany A, Haudek-Prinz V, Meshcheryakova A, Bileck A, Lamm W, Zielinski C, et al. Extracellular matrix remodeling by bone marrow fibroblast-like cells correlates with disease progression in multiple myeloma. *J Proteome Res*. 2014;13(2):844-54.
29. Storti P, Marchica V, Airoidi I, Donofrio G, Fiorini E, Ferri V, et al. Galectin-1 suppression delineates a new strategy to inhibit myeloma-induced angiogenesis and tumoral growth in vivo. *Leukemia*. 2016.
30. An G, Acharya C, Feng X, Wen K, Zhong M, Zhang L, et al. Osteoclasts promote immune suppressive microenvironment in multiple myeloma: therapeutic implication. *Blood*. 2016;128(12):1590-603.
31. Seckinger A, Meissner T, Moreaux J, Depeweg D, Hillengass J, Hose K, et al. Clinical and prognostic role of annexin A2 in multiple myeloma. *Blood*. 2012;120(5):1087-94.

FIGURE LEGENDS

Figure 1. Staining of fibrillar collagens using Masson's trichrome (blue) of mouse bone marrow samples.

- A. Healthy murine bone marrow.
- B. Multiple myeloma murine bone marrow.

Figure 2. Staining of fibrillar collagens using Masson's trichrome (blue) of human bone marrow samples.

- A. Healthy human bone marrow.
- B. Multiple myeloma human bone marrow.

Figure 3. Proteomic pipeline to characterize the ECM composition of normal and diseased bone marrow samples.

- A. Experimental pipeline.
- B. Western blot to control the efficiency of the decellularization of bone marrow samples. Western blot shows the depletion of intracellular components (GAPDH, histones, Transferrin receptor and vimentin) during the four-step decellularization process. Coomassie-stained gel shows the pattern of migration of proteins from the ECM-enriched samples.

Figure 4. Comparison of the matrisome of normal and diseased bone marrow samples.

- A. Bar chart represents the number of proteins constituting the matrisome of normal, MGUS, newly diagnosed MM, and relapsed MM bone marrow.
- B. Venn diagram illustrated the overlap between the matrisome proteins detected in normal, MGUS, newly diagnosed MM, and relapsed MM bone marrow (Supplementary Table S2).

Figure 5. Gene set enrichment analysis of matrisome gene signature in MM patients.

A. Gene set enrichment analysis (GSEA): demonstrating that (A) ECM proteins seen to be depleted in the bone marrow matrix with disease progression were also significantly down regulated at the gene level in normal donors (left) compared to MM patients (right).

B. Heatmap demonstrating enrichment profile of relevant ECM genes in healthy donors vs. MM patients.

Figure 6: Gene expression of ANXA2 in MM cell lines.

A. Analysis of CCLE MM cell lines (red bars) demonstrating the expression ANXA2 in MM cell lines at the mRNA level.

B. ANXA2 is significantly overexpressed at the mRNA level in MGUS, smoldering MM (SMM), newly diagnosed MM (MM, ndx) and relapsed MM (MM relapse) in comparison to normal donors (ND). Dataset reference: Cancer Res. 2007 Apr 1;67(7):2982-9. (GSE6477)

Figure 7: Gene expression of LGALS1 in MM cell lines.

A. LGALS1 is also significantly overexpressed at the mRNA level in newly diagnosed MM patients compared to normal donors in CCLE dataset.

B. LGALS1 is significantly overexpressed at the mRNA level in MGUS, smoldering MM (SMM), newly diagnosed MM (MM, ndx) and relapsed MM (MM relapse) in comparison to normal donors (ND). Dataset reference: Cancer Res. 2007 Apr 1;67(7):2982-9. (GSE6477)

Figure 8. Expression of ECM proteins in MM patients and impact on overall survival.

A. Co-expression of LGALS1 and ANXA2 in MM patients – data sourced from Oncomine (www.oncomine.org) Mulligan MM gene expression Blood. 2007 Apr 15;109(8):3177-88. Epub 2006 Dec 21.

B. Kaplan-Meier survival proportions analysis of patient outcome data from the GSE2658 MM GEP dataset demonstrating high levels of ANXA2 expression associated with inferior overall survival. Log-rank $P = 4.9e-05$

C. Kaplan-Meier survival proportions analysis of patient outcome data from the GSE2658 MM GEP dataset demonstrating high levels of LGALS1 expression associated with inferior overall survival. Log-rank $P = 0.051$.

Supplementary Table S1. Bone marrow matrisome. Matrisome of the bone marrow from healthy donors (A), MGUS patients (B), newly diagnosed multiple myeloma patients (C), and relapsed multiple myeloma patients (D). * indicates ECM or ECM-associated proteins not detected before in any human tissue matrisome.

Supplementary Table S2. Comparison of the matrisome of normal, MGUS, newly diagnosed MM, and relapsed MM bone marrow

Supplementary Table S3. Proteomic data

A. Complete proteomic dataset. Proteins are sorted by matrisome categories and then by Entrez Gene Symbol.

B-E. The total precursor-ion intensity, number of spectra and unique peptides were calculated for each protein and in each sample. Proteins are sorted by number of observations (column D), then matrisome categories (column B) and gene symbols (column C). Proteins detected in at least 3 patients and with at least 3 peptides in one of the samples compose the matrisome of each of the four bone marrow sample types (bold).

B. All ECM and ECM-associated proteins detected in normal bone marrow samples.

C. All ECM and ECM-associated proteins detected in bone marrow samples from MGUS samples.

D. All ECM and ECM-associated proteins detected in bone marrow samples from newly diagnosed multiple myeloma patients.

E. All ECM and ECM-associated proteins detected in bone marrow samples from relapsed multiple myeloma patients.

F. Name of raw mass spectrometry files.

Supplementary Figure 1: Proteomic metrics.

Pie charts represent relative amount of core matrisome (blue), matrisome-associated (orange) and other (grey) proteins in terms of peptide abundance, and numbers of spectra, unique peptides and proteins.

A. Metrics for representative normal bone marrow sample.

B. Metrics for representative MGUS sample.

C. Metrics for representative newly diagnosed multiple myeloma sample.

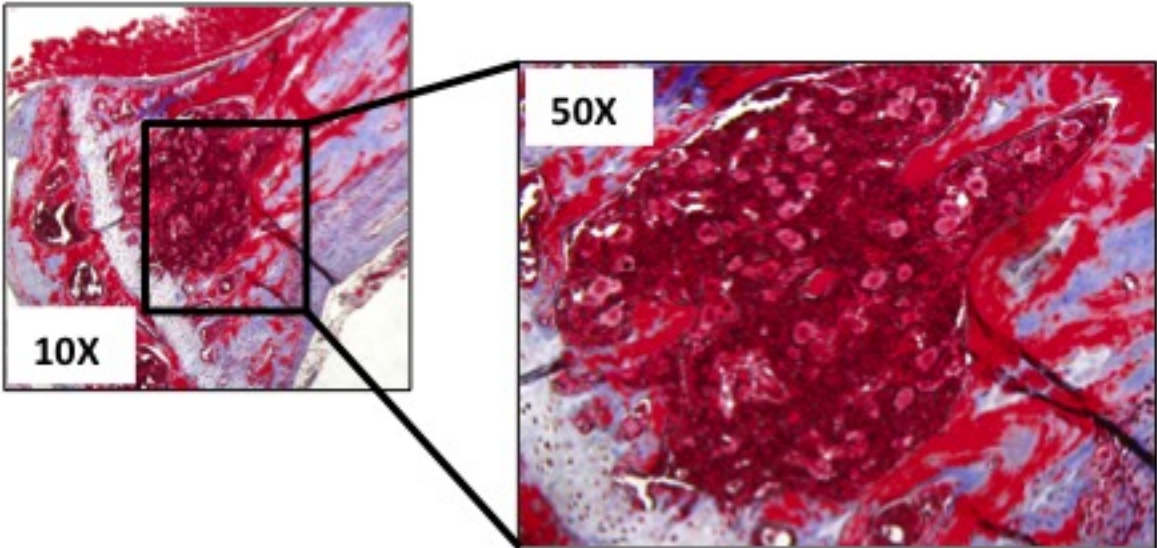
D. Metrics for representative relapsed multiple myeloma sample.

Supplementary Figure 2: ECM peptide abundance

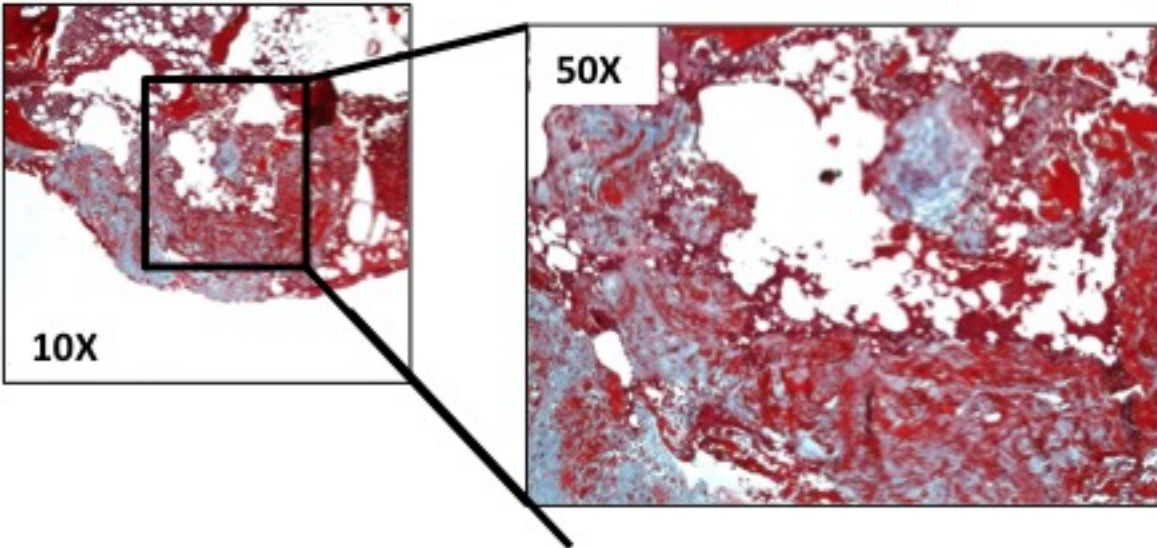
Bar charts represent the peptide abundance for ECM vs non-ECM proteins (**A**) and for core matrisome and matrisome-associated proteins (**B**) in each sample analyzed.

Figure 1

A.
Healthy murine bone marrow



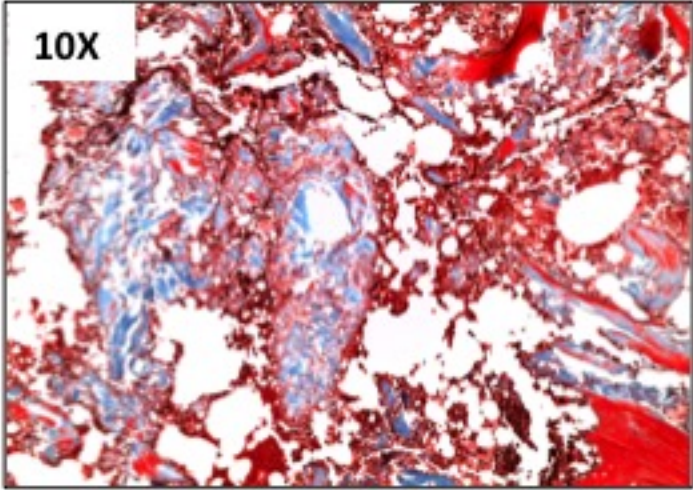
B.
Multiple myeloma murine bone marrow



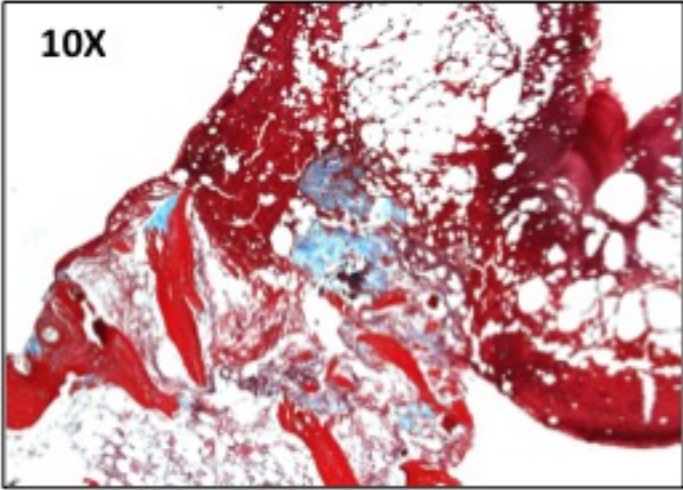
A.

B.

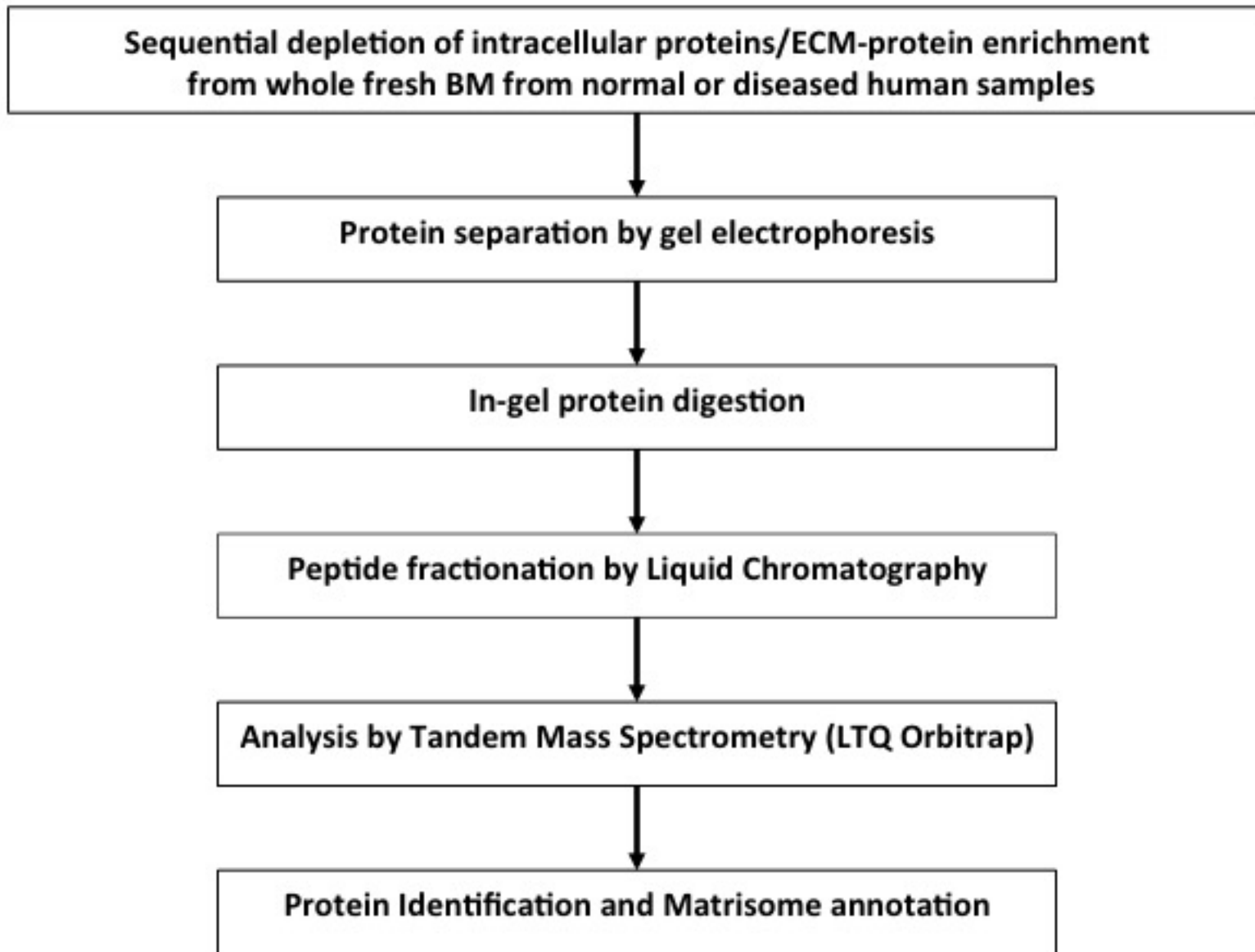
Healthy human bone marrow



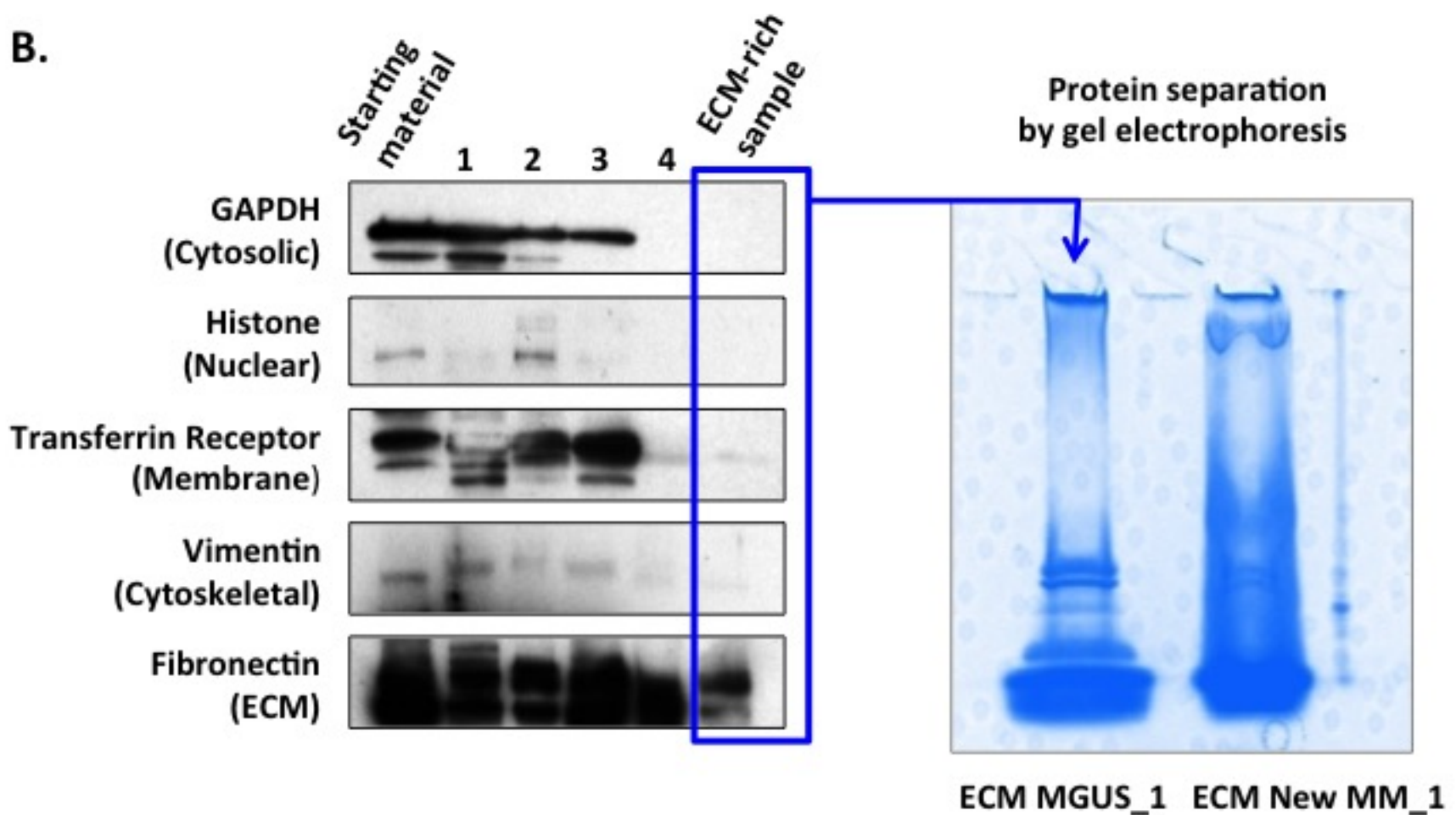
Multiple myeloma human bone marrow



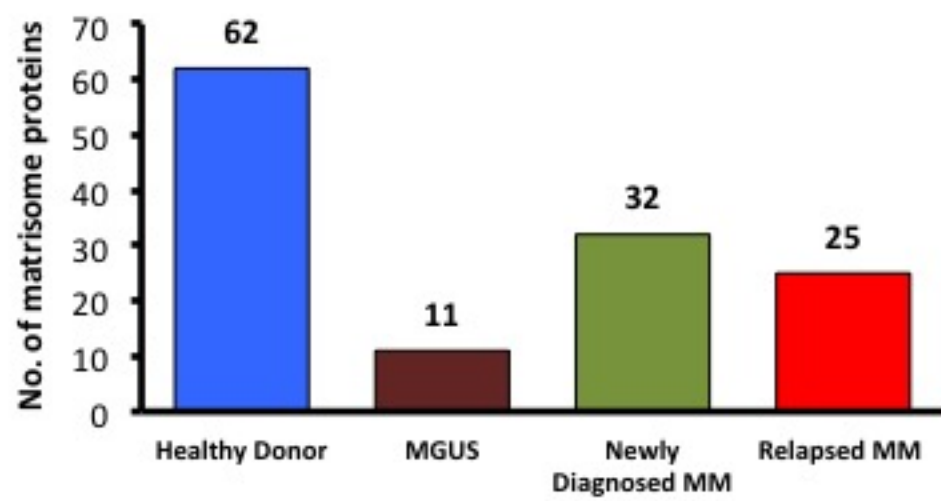
A.



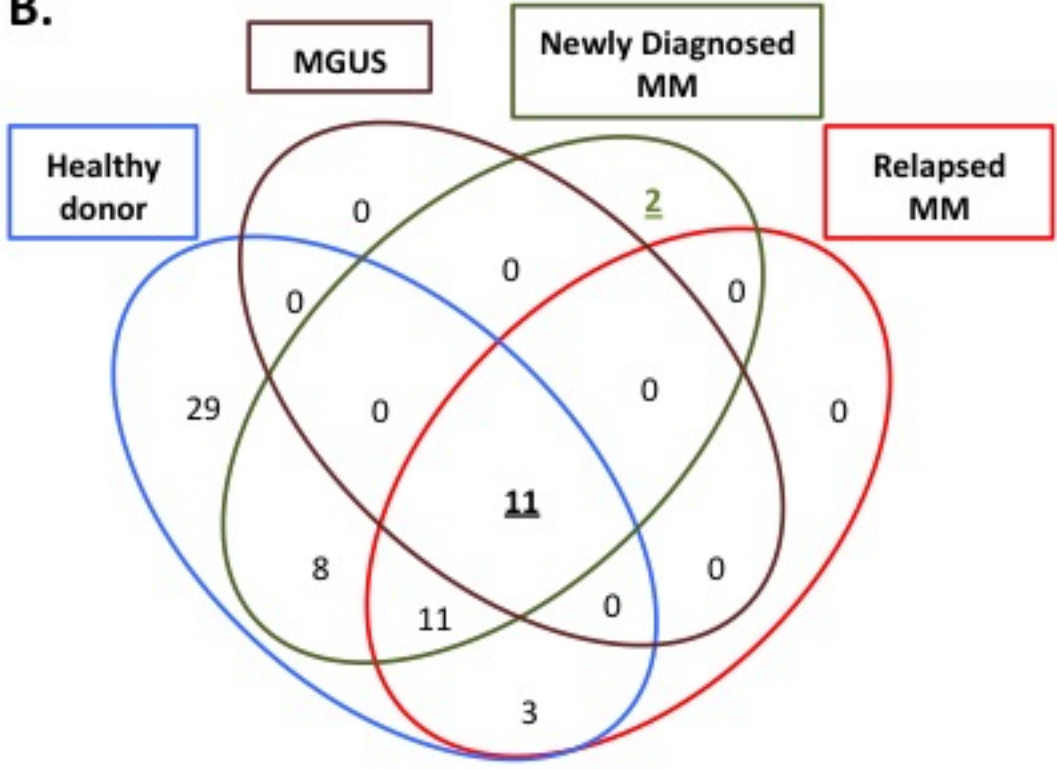
B.



A.

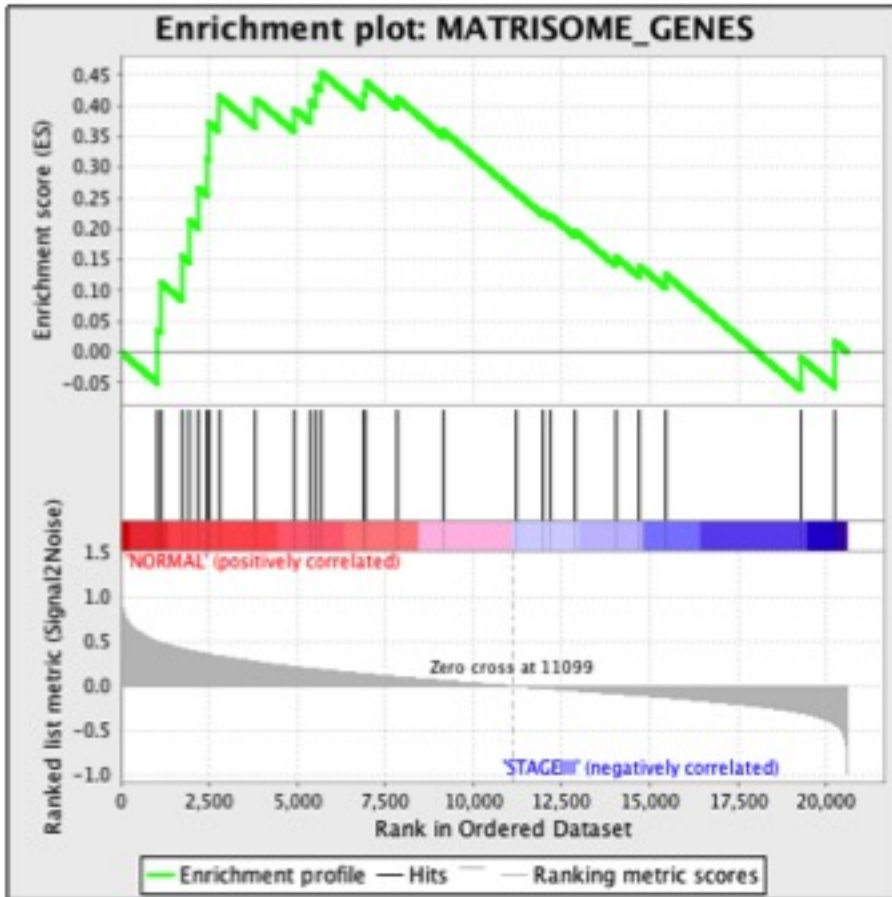


B.



A.

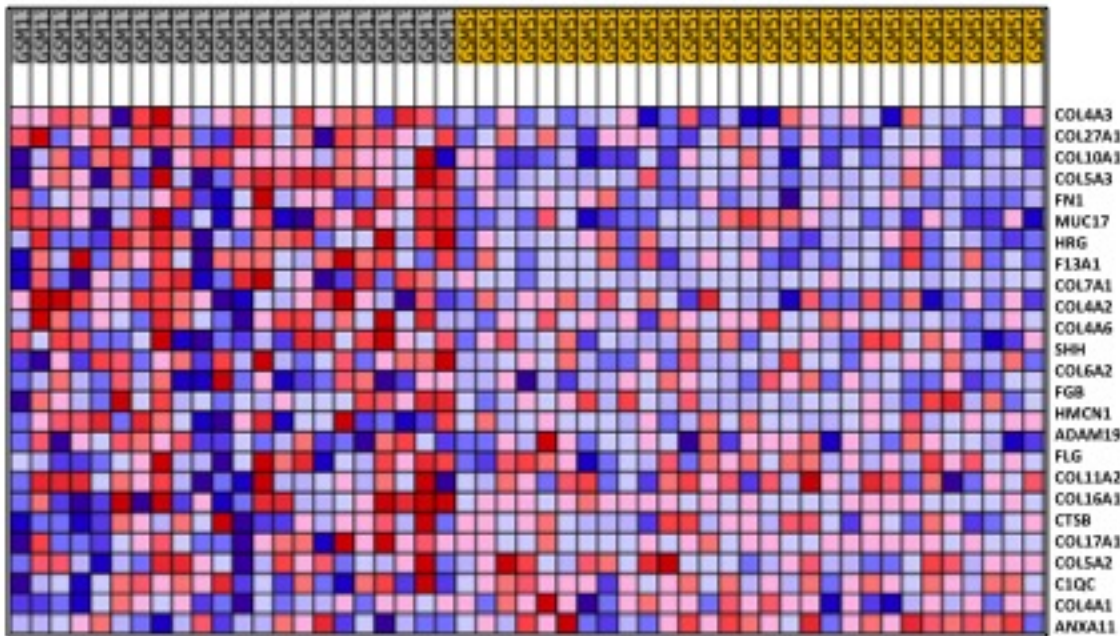
FDR q-value 0.20041323



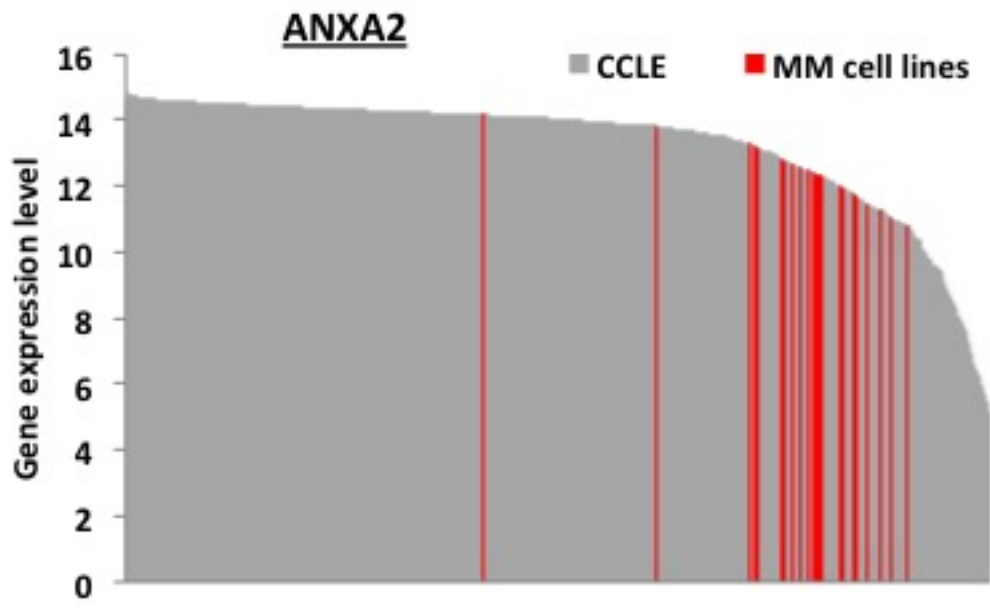
B.

Normal Donor

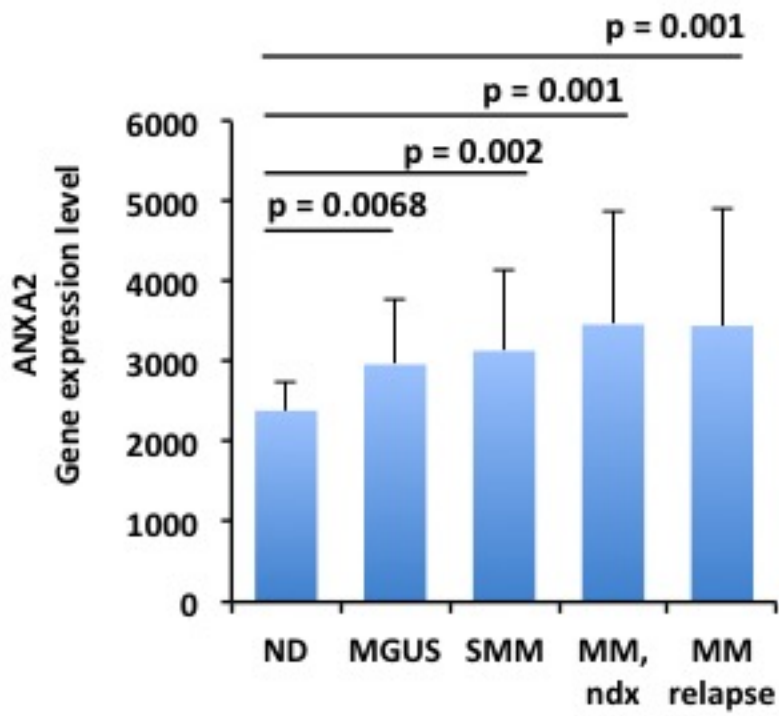
MM patient



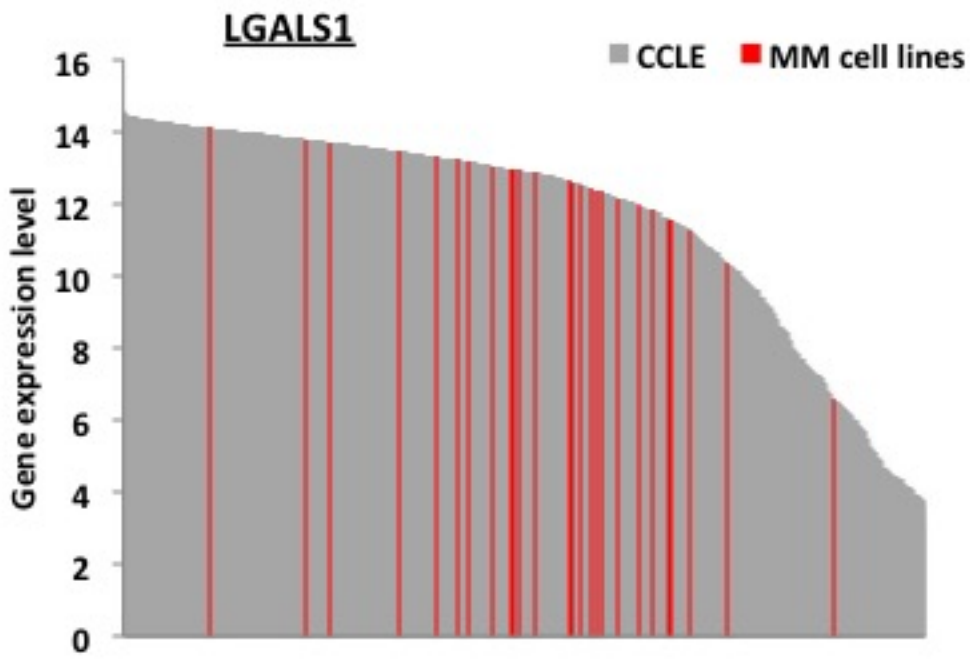
A.



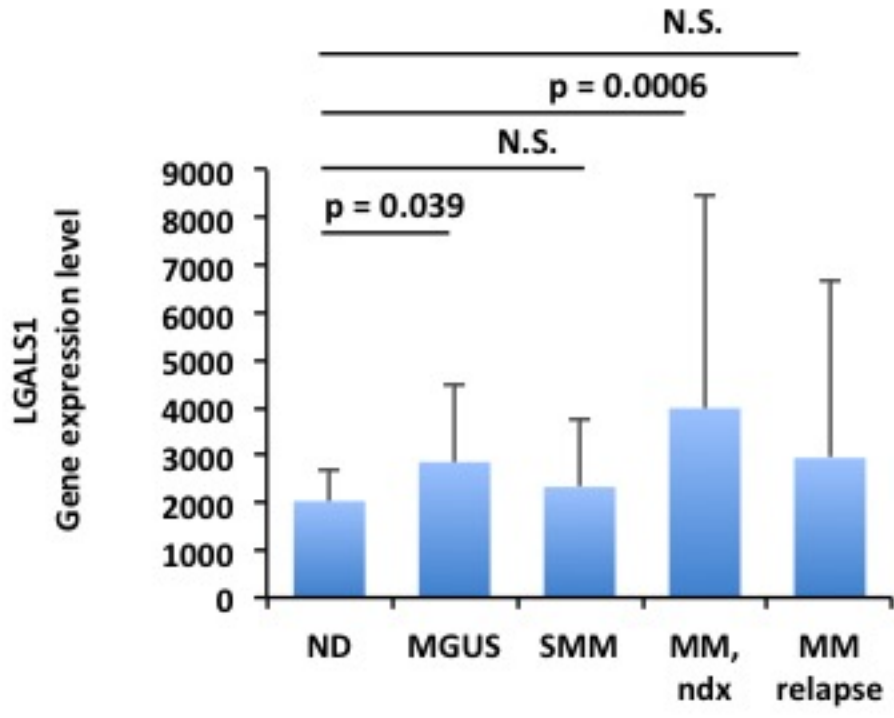
B.



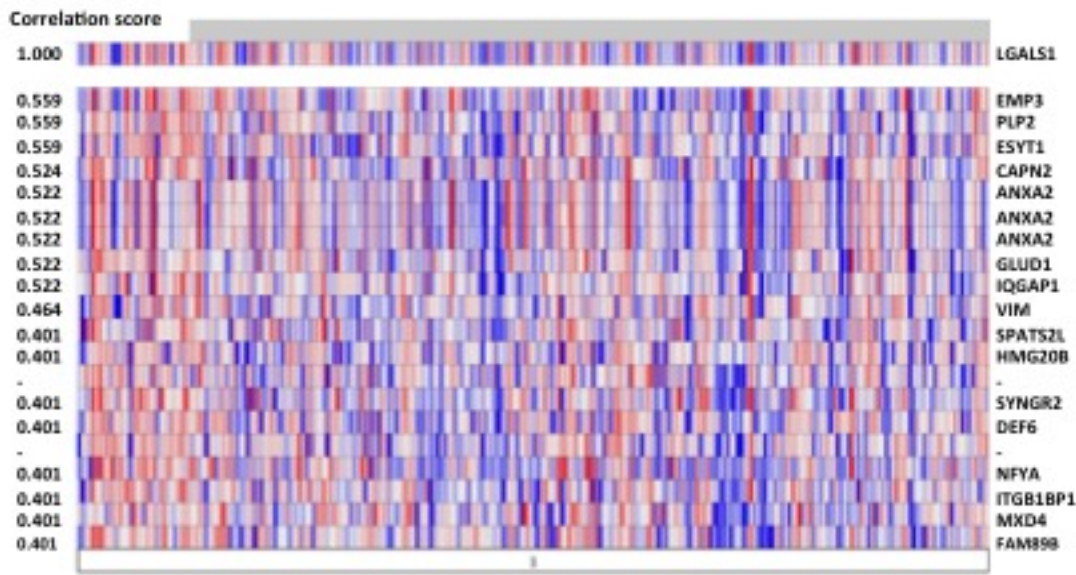
A.



B.

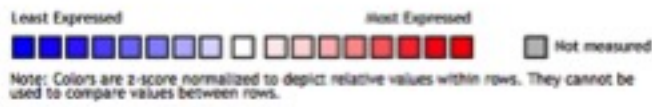


A.

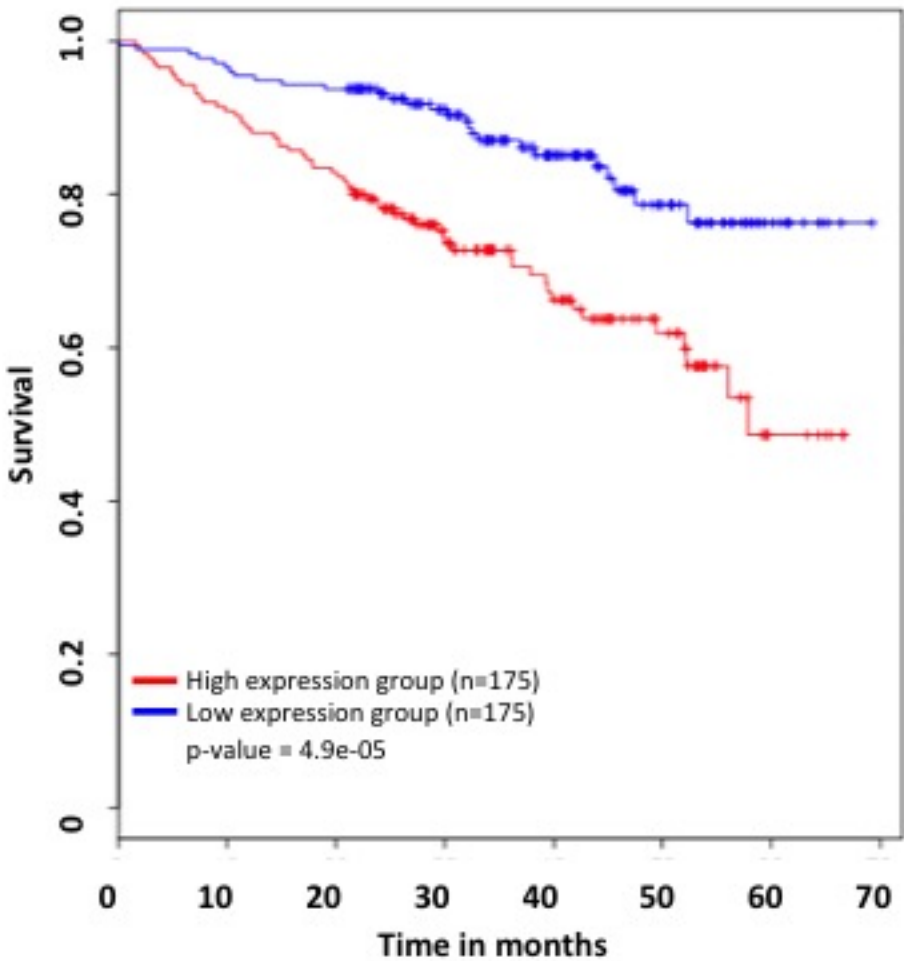


Legend

1. Multiple Myeloma (264)



B. Overall survival MM patients – high vs. low ANXA2



C. Overall survival MM patients – high vs. low LGALS1

